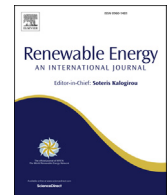




ELSEVIER

Contents lists available at ScienceDirect

Renewable Energy

journal homepage: www.elsevier.com/locate/renene

Techno-economic and exergy analysis of tank and pit thermal energy storage for renewables district heating systems

Abdulrahman Dahash ^{a, b,*}, Fabian Ochs ^a, Alice Tosatto ^a^a Unit of Energy Efficient Buildings, Department of Structural Engineering and Material Sciences, University of Innsbruck, Innsbruck, Austria^b Sustainable Thermal Energy Systems, Center for Energy, AIT Austrian Institute of Technology GmbH, Giefinggasse 2, 1210 Vienna, Austria

ARTICLE INFO

Article history:

Received 26 May 2021

Received in revised form

22 July 2021

Accepted 26 August 2021

Available online 1 September 2021

Keywords:

Seasonal thermal energy storage

Renewable district heating

Techno-economic assessment

Planning and construction

Levelized cost of stored heat

Exergy analysis

ABSTRACT

Large-scale thermal energy storage (TES) emerges as key for the expansion of renewables-based district heating (R-DH) as it is able to bridge the seasonal gap between the heating demand and the availability of renewable energy resources (e.g. solar energy). This work develops a framework for techno-economic analysis considering several key performance indicators (e.g. energy efficiency, exergy efficiency). As TES systems integrated in DH are typically stratified, the work also examines the TES by means of stratification number and efficiency. The economic feasibility of the TES options is examined via the TES specific investment cost. Then, the work recommends the levelized cost of stored heat (LCOS) as a practical measure for the TES techno-economic feasibility. The outcomes show that the tank has higher performance in terms of efficiency indicators (energy and exergy) and stratification measures, but it is characterized with high specific cost. Yet, the tank LCOS is lower compared to that of the shallow pit due to its low performance and despite its low specific cost. Thus, in order to take advantage of the tank's better performance and shallow pit's lower specific cost, the work proposes a third TES geometry called as hybrid TES that combines both tank and shallow pit. The results reveal the potential of this geometry as it arises as a promising option. Furthermore, the results indicate that the transition to low-temperature R-DH brings technical and economic advantages as the LCOS tends to be lower compared to that of TES installed in high-temperature R-DH. Moreover, the work reveals that due to the importance of increasing the economic feasibility for large-scale TES, it is of crucial to develop new materials and construction methods to ensure cost-efficient insulation of the buried TES.

© 2021 The Authors. Published by Elsevier Ltd. This is an open access article under the CC BY license (<http://creativecommons.org/licenses/by/4.0/>).

1. Introduction

The European Union (EU) has set a milestone of a sustainable society with net-zero emissions for the overall greenhouse gasses (GHG) by the year of 2050 compared to the values recorded in 1990 [1]. This action is indeed attributed to the increasing concerns of the environmental issues and challenges arose by the utilization of the fossil fuels (e.g. natural gas) [2,3]. As a result, it is important to carry out a concrete transition in the energy systems in order to substitute the current energy sources (i.e. fossil fuels) with more sustainable energy resources [4,5].

Given the role played by the heating and cooling sector in EU,

this sector significantly contributes to the total energy demand in EU with a share of around 50%. In this context, a major fraction (74%) of the heating and cooling demand is still met by purely conventional fuels with almost 42% via combustion of natural gas. While the remainder is supplied from low-carbon energy sources. In this context, a share of 12% is provided by biomass resources and another portion of 7% is supplied utilizing nuclear energy. Whereas the residual share (7%) of the EU heating and cooling comes from other renewable energy sources (i.e. solar energy) [6]. Therefore, one of the main challenges in meeting this demand is the decarbonization of this sector, which is strongly reliant on the conventional fuels [7]. Together with the fossil fuels substitution, it is crucial to invest into energy efficiency measures to reduce the overall energy demand in order to achieve the EU ambitious goal by 2050.

The buildings sector represents one of the major energy consumers in the EU and it accounts for more than 40% of the total energy demand whereby a major contribution is attributed to the

* Corresponding author. Unit of Energy Efficient Buildings, Department of Structural Engineering and Material Sciences, University of Innsbruck, Innsbruck, Austria

E-mail addresses: Abdulrahman.Dahash@ait.ac.at, Abdulrahman.Dahash@uibk.ac.at (A. Dahash).

Nomenclature		Abbreviations
<i>Symbol</i>		
A	Cross-section area, [m^2]	ATES Aquifer thermal energy storage
ANF	Annuity factor, [%]	BTES Borehole thermal energy storage
C	Cost, [€]	CAPEX Capital expenditure
c	Specific cost, [€/ m^3]	CFD Computational fluid dynamics
c_p	Specific heat capacity, [$\text{J}/(\text{kg.K})$]	CHP Combined heat and power
dz	Incremental length, [m]	DH District heating
E	Energy content, [J]	EU European Union
EX	Exergy, [MWh]	GHG Greenhouse gases
H	Height, [m]	HT High temperature
I	Investment, [€]	H/d Height to diameter ratio
i	Representative segment, [–] or interest rate, [%]	HTC Heat transfer coefficient
L	Service lifetime, [years]	LT Low-temperature
LCOS	Levelized cost of stored heat, [€/MWh]	OPEX Operational expenditure
M	Moment of energy, [J.m]	PTES Pit thermal energy storage
MIX	Mix number, [–]	R-DH Renewable-based district heating
n	Number of segments, [–]	SA/V Surface area to volume ratio
Q	Heat, [J]	S-DH Solar-assisted district heating
\dot{Q}	Heat flowrate, [W]	STES Seasonal thermal energy storage
\dot{q}	Heat flowrate per unit length, [W/m]	TES Thermal energy storage
r	Radius, [m]	TTES Tank thermal energy storage
S	Entropy, [J/K]	
\dot{S}	Rate of entropy, [W/K]	
SA	Surface area, [m^2]	
$\text{Str}(t)$	Stratification number, [–]	
T	Absolute temperature, [K]	
t	Time, [s]	
U	Overall heat transfer coefficient, [W/($\text{m}^2 \cdot \text{K}$)]	
V	Volume, [m^3]	
\dot{V}	Volume flowrate, [m^3/s]	
X	Thickness, [m]	
z	Vertical coordinate inside the tank that corresponds to the distance of the center of a node from the bottom of the tank, [m]	
<i>Greek Symbols</i>		
α	Slope, [$^\circ$]	
Δ	Difference, [–]	
η	Efficiency, [%]	
ϑ	Temperature, [$^\circ\text{C}$]	
λ	Thermal conductivity, [W/(m.K)]	
ρ	Density, [kg/m^3]	
Ψ	Exergy efficiency, [%]	
<i>Subscripts</i>		
0	Initial, or reference	
a	Annual	
bot	Bottom	
ch	Charge	
dest	Destruction	
dis	Discharge	
E	Energy	
eff	Effective	
exp	Experimental	
g	Ground	
gen	Generation	
in	Inlet	
ins	Insulation	
max	Maximum	
min	Minimum	
O&M	Operation and maintenance	
out	Outlet	
RE	Renewable energy	
side	Side	
TES	Thermal energy storage	
top	Top	
w	Water	

heating and cooling activities [8]. Therefore, energy efficiency measures are presented in order to promote the buildings into more energy-efficient ones. As a result, the total energy demand was reduced by approximately 9% in the residential buildings over the last decade [9]. Yet, there exists an increase in the average energy consumption by 0.4% per year [10].

Consequently, the heating and cooling sector shows an enormous potential to carry out further energy reduction by enabling efficiency measures, high shares of renewables and sector coupling in order to further decarbonize the sector. One of the effective key measures is the district heating concept [11,12], which provides heat more efficient than a decentralized/conventional system [8]. Besides, it allows to integrate the renewables leading the fossils to phase-out and, thus, supplying heat at lower costs. Yet, renewables

are intermittent resources and, accordingly, they vary with seasonal and daily patterns [13]. For instance, a mismatch between the energy demand and supply is frequently observed when solar energy is integrated as the solar heat availability peaks during summer, whereas the heating demand is often experienced during winter. Thus, renewables' integration might lead to some risks in energy trilemma (i.e. security of supply) [14].

Accordingly, DH systems should always be flexible and in operation to satisfy the heat demand where and when it is needed [15]. Combined heat and power (CHP) plants represent a key solution as they emerge as a complementary system to support the renewables integration into DH system [16]. Yet, CHPs utilize conventional fuels and, thus, emissions are produced; subsequently, a sustainable option is required. Hence, thermal energy storage

technology is employed as a pivotal component that can bridge the gap between the energy demand and supply, boost the energy system's flexibility and further facilitates the sector-coupling [17].

Thermal energy storage (TES) emerges as an effective player in the energy transition to renewables-based heat supply [18]. Thanks to TES capability in storing heat and making it available on-demand, it concretely assists in the establishment of the so-called renewables-based district heating (R-DH) systems whereby large shares of the renewables are anticipated for integration [19].

The seasonal thermal energy storage (STES) has recently become an inherent component in R-DH systems and the most widely projected TES type for these systems [20–22]. This is due to the capability of the seasonal TES systems to store the thermal energy for lengthy time horizons (e.g. several months) [23]. Besides, this is ascribed to the fact the increase in the TES volume induces a notable reduction in the thermal losses due to the good surface area-to-volume ratio (SA/V) [24]. As large-scale seasonal TES systems store energy for lengthy timescales, it is essential to locate such systems properly as they require large space availability. Subsequently, the STES systems are commonly planned for installation in the subsurface (partially or fully buried in the ground), where the temperature varies less than that in the ambient. Literature classifies the most common STES types of STES as follows [19]:

- i. Aquifer TES (ATES);
- ii. Borehole TES (BTES);
- iii. Tank TES (TTES); and
- iv. Pit TES (PTES).

The ATES and BTES systems are often exploited whereby moderate charging/discharging energy rates are observed in the boundary conditions of the operation (low temperature and moderate flowrates). On the contrary, hot-water tanks and pits are prominent for their competence to achieve high charging/discharging energy rates.

Further, the larger the TES volume, the cheaper are the specific capital cost ($\text{€}/\text{m}^3$) under the same structural and construction boundary conditions [25] as established in Figs. 1 and 2, which reveals the investment cost for a number of realized large-scale TES systems. The data includes two TES types, which are shallow pit and tank. For a peer-to-peer comparison, Fig. 1 shows the TES specific cost related to the water equivalent TES volume. It must be mentioned that Fig. 1 confirms the economy of scale for such

systems. Therein, the curve shown is formed for the shallow pits installed in Denmark [26].

In order to obtain the ultimate advantages of STES, it is essential to properly design, effectively plan and adequately size these systems with their relevant components (e.g., charging/discharging devices, insulation thickness) [19]. Subsequently, planning and construction of large-scale R-DH coupled with seasonal TES is a complex process. This arises from the fact that the planning process is an interconnected sophisticated process due to the number of factors (e.g. location, hydrogeological conditions, TES construction type, TES size, TES geometry, storage medium and others) that have to be included in the process as illustrated in Ref. [19]. Nevertheless, it is hardly feasible to construct pilot TES projects with large-scale volumes to conduct experiments due to the enormous capital cost. Besides, another risk is the potential of low TES performance. Therefore, calibrated STES and system simulations found their place favorably to examine the planning and operation of large-scale systems [28]. Thus, the simulation results of numerical models are often compared to monitoring data from demonstration projects.

Hence, this work emphasizes the importance of a techno-economic evaluation framework that is able to capture all the related aspects of STES and systematically quantifies its impact. This work presents a techno-economic metric that reflects the impact of the total STES cost (i.e. capital expenditure, operation and maintenance costs) on the amount of the delivered heat. This metric is the leveled cost of stored heat, which will be used in order to establish STES planning guidelines. By virtue of this metric, a list of STES geometries and volumes will be compared. Further, this measure will assess in the impact evaluation between a low-temperature (LT-DH) and a high-temperature district heating (HT-DH). Thus, the authors present numerical models appropriate for simulations of large-scale TES (e.g. tank, conical pit, pyramid stump pit) in renewables-based DH systems.

In this work, the authors report the advances, challenges and solutions in planning and construction of large-scale TES considering a number of studies and projects. The work reviews a number of studies investigated the role of large-scale TES geometry on temperature stratification and exergy losses. By addressing the shortcomings in other studies, the authors suggest a methodology for techno-economic analysis and exergy assessment for large-scale tank and pit TES. This work's novelty is the establishment of techno-economic planning guidelines considering several factors affecting TES systems. Such factors are the TES geometry, H/d ratio,

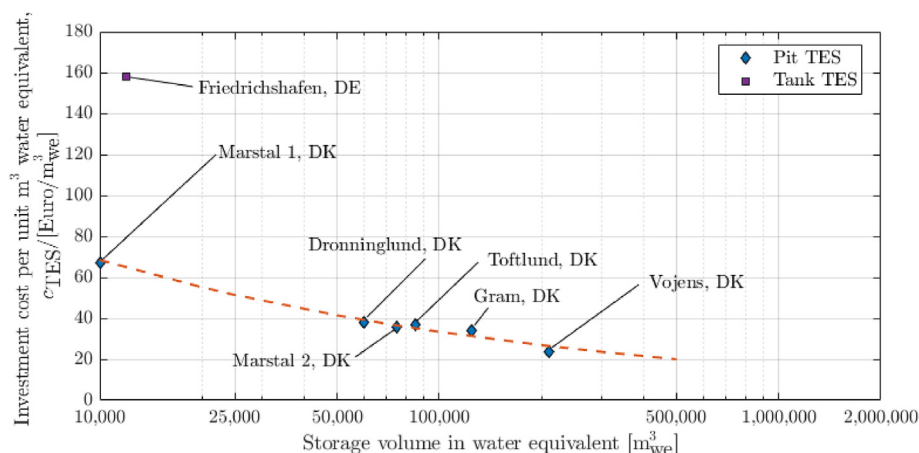


Fig. 1. Specific investment cost for large-scale TES systems related to the TES volume in water equivalent (reproduced from Ref. [27]). (Costs are without value added taxes. Costs include construction of TES and exclude planning cost, connecting pipes and heating plants equipment [27]).

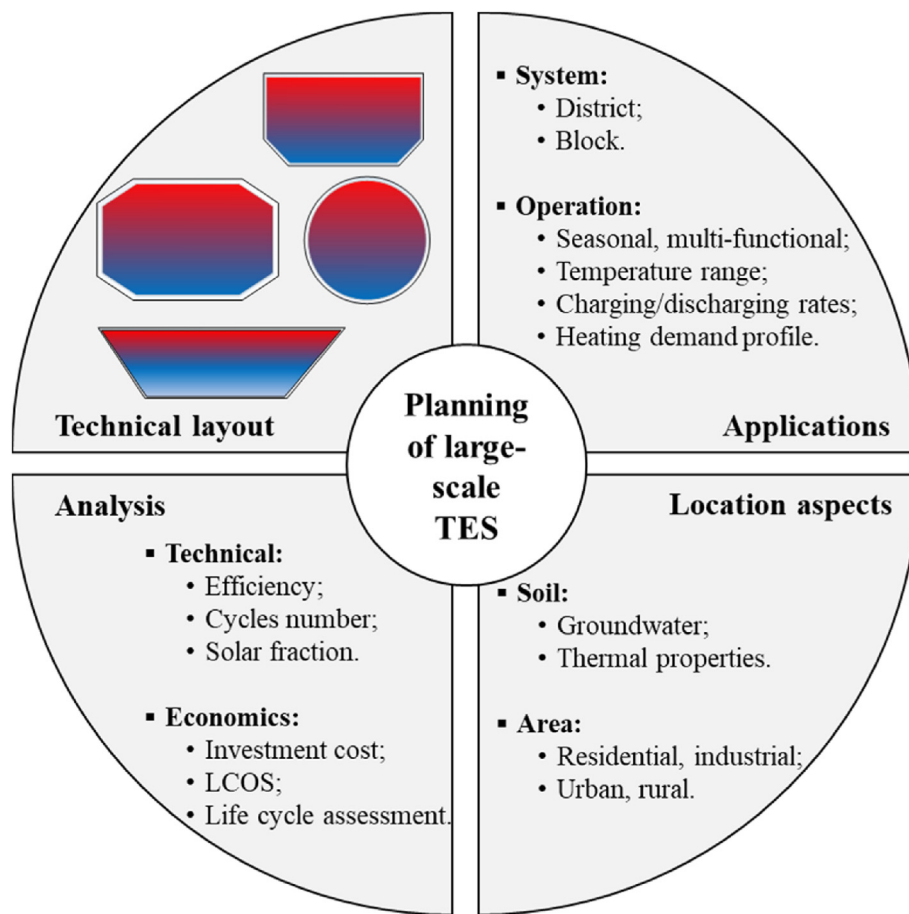


Fig. 2. A number of influencing parameters on the planning layout of large-scale underground TES and its economic feasibility (reproduced from Ref. [19]).

SA/V ratio, insulation level and quality, TES size and DH characteristics. Such guidelines will provide the researchers and planners with insights in order to arrive at TES optimal planning when aiming at renewables-based district heating systems.

2. State of the art in seasonal and large-scale TES

Seasonal thermal energy storage gradually emerges as a key component for the implementation of renewables-based district heating systems as it is aimed to mitigate CO₂ emissions and alleviate the climate change. Large-scale TES systems store the thermal energy for lengthy periods; therefore, such systems must be properly located as they require large space availability. Hence, seasonal thermal energy storage systems are frequently installed in the subsurface. Given the fact that tank and pit TES are able to store heat up to a temperature of 95 °C and, thus, they realize high rates for charging/discharging, this work excludes the aquifers and boreholes from the examination and this results in a focus toward tank and pit TES as they are favorable for R-DH [29].

2.1. Planning and construction of large-scale seasonal TES

Given the desired expansion in renewables energy share and down to their volatile character, a great focus on large-scale hot water tank and pit TES has been paid. Within this attention shall not only the operation of such systems be considered but also their design and layout. In particular, the planning and construction phases have been at the spot in an increasing number of research

and development activities. This awareness is strongly ascribed to the fact that large-scale TES systems demand a space availability due to the substantial great volume required to efficiently accomplish the long-term storage [19]. Therefore, it is important to address all the relevant questions during the planning phase when seeking the optimal TES for a specific R-DH system. Otherwise, the capital investment cost might be lost when the TES performance is below expectations and the goal (e.g. abatement of CO₂ and reduction of fossils) is not achieved. Such questions usually concern a group of players that might have an impact of TES techno-economic performance. These questions include hydrogeological conditions (e.g. soil type, groundwater existence and/or flowing), TES geometry (e.g. tanks, conical pits, pyramid stump pits), TES construction (e.g. freestanding, partially or fully buried), system characteristics (e.g. operation temperatures), liners and insulation and others. In this context, large-scale TES planning and construction dependency on these questions and others is revealed in Ref. [19]. It is found that addressing answers to these questions play a critical role in the techno-economic assessment of such stores. Hence, it is important to strive for an optimal TES selection whereby a compromise between the economic investment and the technical performance is made.

Toward the establishment of a techno-economic analysis methodology, Ochs et al. [29] estimated the investment cost (i.e. capital expenditure) for large-scale TES considering different options in order to establish construction guidelines. The options included TES volumes in the range of 100,000 m³ up to 2,000,000 m³ for shallow pits and tanks. The study revealed that

shallow pits planned with floating covers are characterized with cheaper specific capital cost compared to that of the tanks. Yet, if the concept includes a trafficable cover, then the feasibility of shallow pits drops and they are accordingly eliminated from the TES selection plan. Further, the work proved the role of DH characteristics on the TES performance concluding that large-scale TES installed in LT-DH systems have better both technical performance and economic feasibility with regards to their corresponding installed in HT-DH systems.

In an attempt to set a framework for sustainability assessment of R-DH system, Abokersh et al. [20] investigated the optimal integration of solar-assisted district heating system (S-DH) for different urban sized communities. There, the work paid notable attention toward multi-objective optimization of such systems. Besides, it paid noteworthy efforts towards developing a robust machine learning model to tackle the computational challenges associated in optimization problems for TRNSYS models. The aim of the work was the inspection of techno-economic-environmental feasibility for S-DH. The work considered a partially-buried seasonal TES with a circular cross-section and a geometry shown in Fig. 3(c). Yet, the work did not thoroughly investigate the techno-economic planning of the TES considering different construction types and geometries. Instead, the work investigated the influence of different insulation materials (i.e. mineral wool, extruded polystyrene, foam glass gravel) and construction materials (i.e. normal concrete, high-performance concrete, ultra-high-performance concrete) on the S-DH performance due to STES thermal losses. Whereas the TES volume ranged between 1 m³ and 100,000 m³.

2.2. Impact of large-scale seasonal TES construction on performance and stratification

In a TES system, the thermal stratification refers to the distribution of the storage medium into sequential volumes with different temperatures along the TES height regardless of TES orientation and this is due to the action of buoyancy force (i.e. the inclusion of gravitational acceleration). Thereby, the hot water tends to accumulate at the top of the TES, whereas lukewarm water is accordingly forced to move downwards gathering at the bottom of the TES. Undoubtedly, thermal stratification decays over time due a number of inducing parameters: 1) heat loss (or gain as well) to the surroundings of the TES; 2) conductive heat transfer through the TES lateral wall; 3) conductive and natural convective heat transfer processes between each two adjacent stratified TES segments; and 4) forced mixing due to the induced local turbulence by the rapid increase of the kinetic energy during charging/discharging phases.

Accordingly, it is important to mention that the latter mechanism (i.e. forced mixing during charging/discharging) calls the necessity for designing the inlet diffusers properly. Whereas it is well known that the other mechanisms are strongly related to the

TES geometrical parameters. In this context, it is fundamental to mention that the TES aspect ratio (i.e. height-to-diameter ratio) and TES geometry arise as key players in thermal stratification.

In this regard, Panthalookaran et al. [30] examined the influence of aspect ratio, store shape, TES internal structure and TES volume on thermal stratification by means of developed numerical CFD models. Therein, the investigated TES volume varied between 2500 m³ and 12,000 m³, whilst the aspect ratio was in the range of 0.5 up to 3. Given the fact that spherical TES shapes outperform other options due to the possibly lowest surface area-to-volume ratio, the work discussed and compared different store shapes shown in Fig. 3. The study found that slopped-wall bottom TES tends to outperform other shapes. Further, the study addressed a new characterization method for the assessment of thermal stratification in large hot water TES. The method incorporated the minimization of entropy generation.

By virtue of computational fluid dynamics (CFD), Chang et al. [31] addressed the influence of characteristic parameters (e.g. TES height, TES slope angle) on the thermal stratification of PTES (i.e. truncated pyramid stump). There, the key outcomes revealed that the decrease in the PTES height led to a decrease in the degree of stratification and, therefore, less thermal efficiency. For the assessment, thermal efficiency indicator and TES average temperature over TES dimensionless height were used.

Furthermore, Park et al. [32] investigated the thermal behavior of stored hot water in underground rock caverns exploited as large-scale TES. For this purpose, Lyckebo rock cavern in Sweden was used as a case study with a volume of 100,000 m³. Therein, the work highlighted that the aspect ratio and the heating of the surrounding rocks were the key players influencing the quality of stratification. For the analysis, the degree of stratification (i.e. Stratification number, $Str(t)$) was utilized.

Moreover, Hahne and Chen [33] numerically demonstrated that the increase of the aspect ratio can significantly improve the TES charging efficiency and thermal stratification. Accordingly, they found that an aspect ratio between 3 and 4 is deemed to be a reasonable compromise for practical TES applications.

It is important to mention that the findings of the aforementioned studies ([31–33]) are mostly based on the 1st law of thermodynamics. The energy efficiency measures are meaningful indices as they offer some insights into the TES design. Yet, it is probable that the planner might miss the entire picture when planning a large-scale seasonal TES due to the high number of influencing parameters [19]. Besides, it is crucial to underline the absence of a comprehensive energy efficiency measure that is capable of capturing also the internal thermal losses in TES. Therefore, the literature addresses several indicators (e.g. MIX number, $Str(t)$, rate of entropy generation).

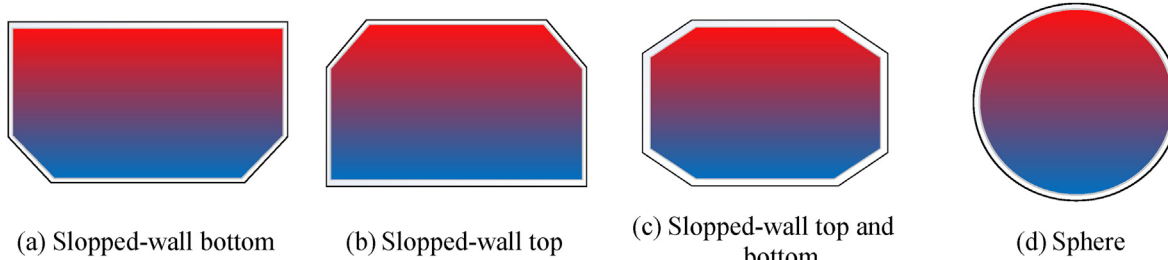


Fig. 3. Possible TES geometries for large-scale applications.

2.3. Contribution and novelty of the work

In this study, the objectives can be listed as below:

- Presentation of a numerical approach for modeling large-scale TES; and
- Examination of the TES geometry impact on stratification by carrying out a technical analysis for two TES geometries (cylindrical tank TES and cone pit TES) as presented in Fig. 4(a) and (b).

On this basis, several key performance indicators are introduced in order to conduct the evaluation. As a result, the work proposes a third TES geometry illustrated in Fig. 4(c), which combines both TTES and PTES configuration in order to obtain the benefits of both geometries. Fig. 4 presents the different TES geometries examined in this work, whilst Table 1, Table 2 and Table 3 report the TES dimensions together with other geometrical characteristics (i.e. H/d ratio, SA/V ratio, TES slope) for the different volumes investigated. It is worthy to point out that [34] considers the groundwater flow in the TES surroundings and attempts to establish techno-economic-environmental guidelines for TES constructions in the subsurface whereby groundwater flow is inevitable. Therefore, it is decided that this work pays more attention to techno-economic guidelines for TES planning under favorable hydro-geological conditions (i.e. no groundwater existence or flowing) and for a given set of boundary conditions for R-DH.

Having considered the anticipated lengthy storage periods in STES (few weeks up to several months), it is essential to design STES systems with favorable aspect ratios and proper geometries. On this basis, exergy efficiency measure emerges as a promising indicator as it is able to capture the influence of mixing losses that are basically temperature losses affecting the quality of discharged amount of heat. Thus, this work will utilize different performance measures (i.e. energy and exergy efficiency) and stratification quality measures (e.g. stratification efficiency, $Str(t)$) when seeking the optimal STES.

Furthermore, the work extends the investigation to a techno-economic analysis framework. Thus, another objective can be listed:

- Report of the leveled cost of stored heat (LCOS) for each TES geometry and volume investigated;

The importance of this indicator (i.e. LCOS) is that it crucially pinpoints the role of TES geometry and volume on the technical performance and the stored heat unit price. Therefore, the novelty of this work is the establishment of techno-economic guidelines for large-scale hot water tanks and pits that will later aid the planners of renewables-based district heating to easily find the optimal TES solutions for the corresponding districts based on several key performance indicators (e.g. energy efficiency, exergy efficiency, stratification quality, LCOS).

3. Methodology

3.1. Numerical modeling of hot-water TES

The optimal design and plan of large-scale seasonal TES requires modeling techniques that can correctly capture the thermo-hydraulics to provide the planners with numerous insights allowing to achieve an optimal layout. Therefore, the multi-physical aspects (i.e. heat and mass transfer, flow dynamics and others) must be included in the numerical model. Accordingly, a TES model developed in COMSOL Multiphysics® is utilized in this work to

represent a list TES shapes (i.e. shallow pit, tank, hybrid, cuboid, etc.). Fig. 5 shows a fully-buried shallow pit with a symmetry plane whereby $r = 0$. Therein, the shallow pit has 3 diffusers (i.e. inlet/outlet port) in order to demonstrate that the model can simulate a TES with several ports. It is important to pinpoint that this work does not present the development of the numerical model as it is extensively presented in a synopsis of studies [35,36], validated in Ref. [26], utilized for investigations on groundwater-TES interaction in the subsurface as in Ref. [23] and used for a techno-economic planning framework in Ref. [29].

For any TES segment (i), heat transfer mechanisms are considered in an energy balance that can be expressed as a partial differential equation as follows:

$$(\rho A_i c_p) \frac{\partial T_i(t)}{\partial t} = -(\rho \dot{V}_w c_p) \frac{\partial T_i(t)}{\partial z_i} + A_i \frac{\partial}{\partial z_i} \left(\lambda_{w,\text{eff}} \frac{\partial T_i}{\partial z_i} \right) - \dot{q}_{\text{loss},i} \quad (1)$$

Where ρ , c_p and $\lambda_{w,\text{eff}}$ represent the density, specific heat capacity and effective thermal conductivity of the storage medium (i.e. water), respectively. Whereas A_i is the cross-section area of the segment (i). Detailed information on the modeling can be found in the aforementioned literature.

In reality, no forced convection mechanism is seen during TES standby phases (i.e. storage and idle). Instead, a buoyancy-driven natural convection heat flow is the leading mechanism. This phenomenon arises from the fact that water has a temperature-dependent density. Consequently, the water buoyancy induces a natural convection process. Given the relatively high thermal losses through the top of TES, a temperature decrease can be notable near to the upper surface area of the TES (at the very top). As a result, an unrealistic behavior known as “inverse thermocline” can be seen in the simulated stratification profile.

To tackle this shortcoming, the water thermal conductivity encompasses the nominal value and the effective value to enhance the thermal conductivity; consequently, eliminate inverse thermocline. Accordingly:

$$\lambda_{w,\text{eff}} = \begin{cases} \lambda_w, & |\dot{V}_w| \neq 0 \\ \lambda_w + C \cdot \left(\left| \frac{\partial T_i}{\partial z_i} \right| \right)^k, & \left| \frac{\partial T_i}{\partial z_i} \right| < 0 \end{cases} \quad (2)$$

Where the term $(C \cdot \left(\left| \frac{\partial T_i}{\partial z_i} \right| \right)^k)$ stands for the enhanced thermal conductivity, which is based on Nusselt and Rayleigh numbers and, accordingly, adjusted based on the basis of the considered application (large-scale TES). Here, C represents a constant that combines the influence of geometrical parameters (e.g. volume, height) with thermo-physical properties (e.g. density, specific heat capacity). Whilst k is adjusted following the application; however, in this case $k = 0.5$.

It is essential to compare the obtained results from the developed numerical model against a set of measured data in order to verify the model's applicability and to attain credibility in the developed model. Therefore, the study [26] is recommended as it reports the details of model development and documents the calibration of the model.

3.2. Operation scenarios, assumptions and boundary conditions

In this research, the focus is to develop STES models that are reliable and computationally fast enough to give insights on the design of STES. Therefore, system simulations are not considered at

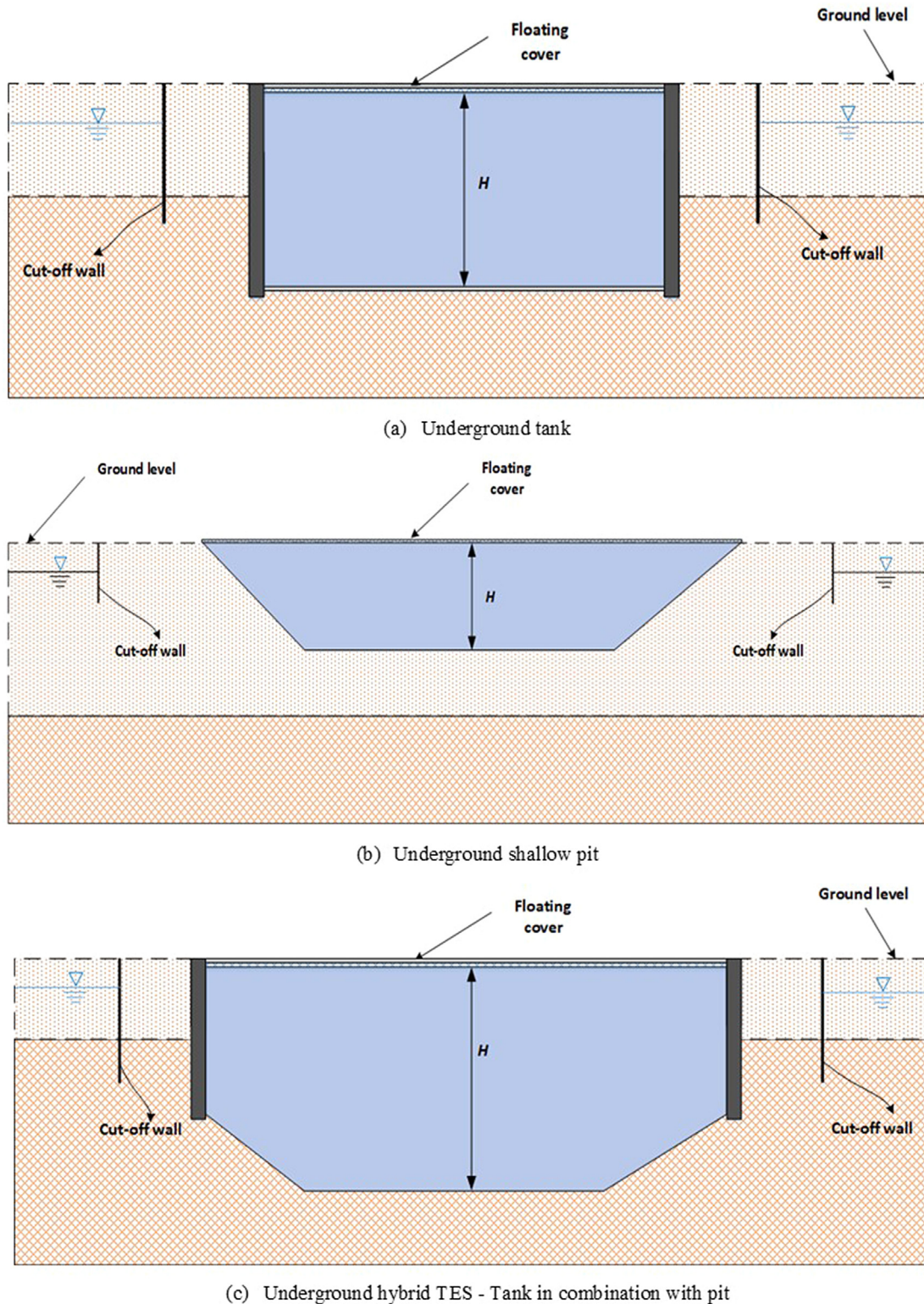


Fig. 4. Different geometries and construction types considered in this work.

this stage and this means no DH system is actually modeled. Nevertheless, the DH operation profiles (temperature and flowrate) are pivotal for the operation of STES system (i.e. charging and discharging). Therefore, a simplified standard DH temperature profile is introduced in the model, where 90 °C and 60 °C are the DH supply and return temperature, respectively. Fig. 6 and Fig. 7 show

the simplified periodic operating conditions for a TES. Table 4 reports the thermo-physical properties and other significant parameters used for the simulations.

Table 1

Tank TES dimensions for the different volumes investigated in this work.

	Case 1	Case 2	Case 3	Case 4	Case 5
Height, H [m]	50	50	50	50	50
Diameter, d [m]	50.46	71.36	112.83	159.57	225.67
Surface area, SA [m^2]	11,927	19,210	37,725	65,066	115,449
Volume, V [m^3]	100,000	200,000	500,000	1,000,000	2,000,000
H/d [-]	0.991	0.701	0.443	0.313	0.222
SA/V [1/m]	0.119	0.096	0.075	0.065	0.058
Slope, α [$^\circ$]	90	90	90	90	90

Table 2Shallow pit TES dimensions for the different volumes investigated in this work^a.

	Case 1	Case 2	Case 3	Case 4	Case 5
Height, H [m]	10.5	11.8	13.8	15.6	17.7
Top diameter, d [m]	127.8	167	238.3	312.2	409.5
Bottom diameter, d [m]	91.4	126.2	190.5	258.1	348.1
Surface area, SA [m^2]	26,620	45,241	91,669	156,868	268,997
Volume, V [m^3]	100,000	200,000	500,000	1,000,000	2,000,000
H/d [-]	0.096	0.08	0.064	0.055	0.047
SA/V [1/m]	0.266	0.266	0.183	0.157	0.134
Slope, α [$^\circ$]	30	30	30	30	30

^a The authors chose these dimensions for the shallow pit configuration by purpose in order to highlight the influence of (H/d) and (SA/V) ratio on the TES energetic and exergetic efficiency (i.e. stratification).

Table 3

Hybrid TES dimensions for the different volumes investigated in this work.

	Case 1	Case 2	Case 3	Case 4	Case 5
Height, H_{pit} [m]	6	6	7	10	12
Height, H_{tank} [m]	11.94	14.17	15	20.4	30.24
Height, H [m]	17.94	20.17	22	30.4	42.24
Top diameter, d [m]	88.25	116	174.45	210	252
Bottom diameter, d [m]	62.36	90	146	176	204
Surface area, SA [m^2]	14,063	26,727	56,842	84,385	125,723
Volume, V [m^3]	100,000	200,000	500,000	1,000,000	2,000,000
H/d [-]	0.24	0.2	0.14	0.16	0.19
SA/V [1/m]	0.16	0.13	0.11	0.08	0.06
Slope, α [$^\circ$]	25	24	26	30	26

3.3. Key performance indicators

For a thorough performance analysis, the methodology

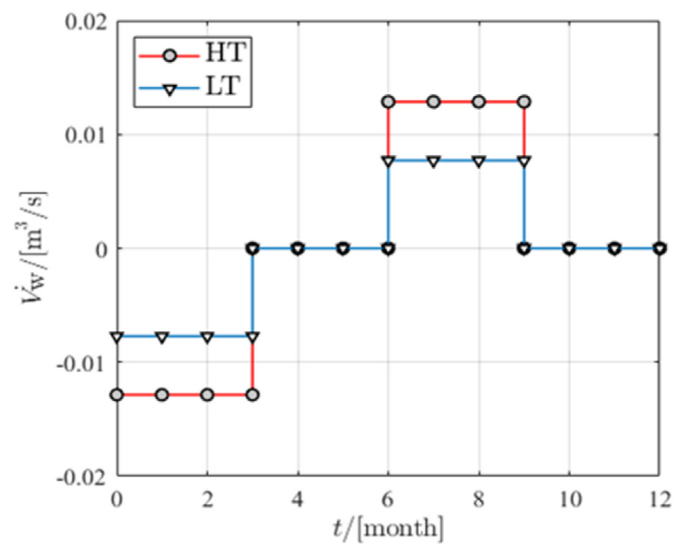


Fig. 6. A year-round incoming/outgoing flowrate for a TES with a volume of 100,000 m^3 . (HT: high temperature, LT: low temperature).

framework must include expressive physics-based quantities that indicate the TES performance of one storage and, subsequently, compare it with another storage to select the optimal TES in the decision-making process. Thus, numerous indicators (e.g. TES energy efficiency, TES stratification, thermocline thickness) are well established and discussed in literature.

3.3.1. Technical key performance indicators

To address TES capability in recovering the energy injected and/or stored, TES energy efficiency is seen as a meaningful indicator since it is based on the 1st law of thermodynamics. Thus, TES energy efficiency depicts the ratio of the TES discharged heat (Q_{dis}) at useful temperature to the total heat input (Q_{ch}) at charging temperature. Accordingly:

$$\eta_I = \frac{Q_{\text{dis}}}{Q_{\text{ch}}} \quad (3)$$

Despite its conventionality, this particular definition shows a sensitivity of TES to the operation parameters (e.g. charging/

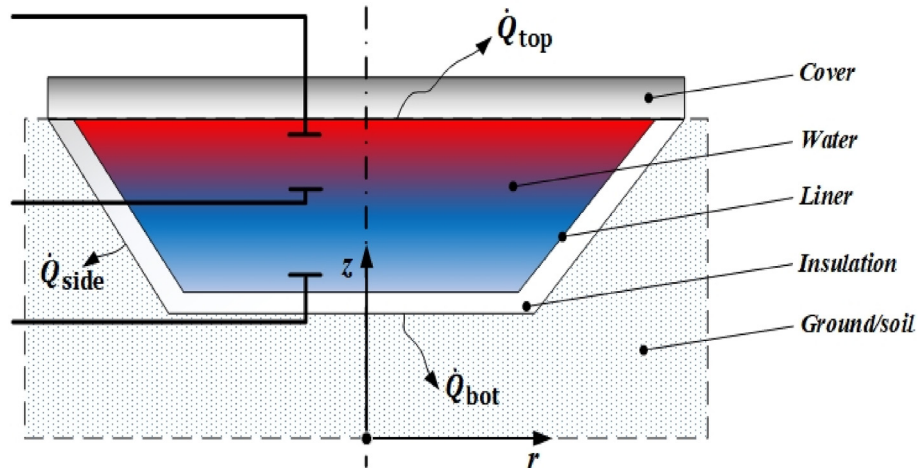


Fig. 5. An exemplary 2-D representation of an underground shallow pit with the different required domains and surroundings [35].

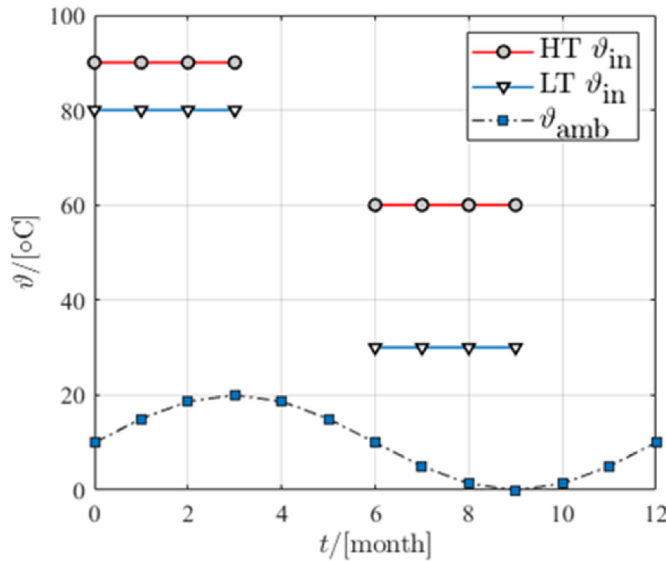


Fig. 7. A year-round injection temperature into TES and ambient temperature as a sinus function with an average of 10 °C. (HT: high temperature, LT: low temperature).

Table 4
Thermo-physical properties of the materials and heat transfer coefficients (HTC) of the different components in TES.

Parameter	Value
Water thermal conductivity, λ_w	0.6 W/(m.K)
Water density, ρ	1000 kg/m ³
Water specific heat capacity, c_p	4200 J/(kg.K)
Overall HTC of the top (cover), U_{top}	0.1 W/(m ² .K)
Overall HTC of the sidewalls, U_{side}	0.3 W/(m ² .K)
Overall HTC of the bottom, U_{bot}	0.3 W/(m ² .K)
Ground thermal conductivity, λ_g	1.5 W/(m.K)
Ground specific heat capacity, $c_{p,g}$	880 J/(kg.K)
Ground density, ρ_g	1000 kg/m ³

discharging). Besides, it does not sufficiently address the TES effective energy capacity related to the thermal losses [19]. Subsequently, another performance indicator is defined, which is TES energy capacity efficiency and obeys the following definition:

$$\eta_{II} = 1 - \frac{Q_{loss}}{Q_{TES}} \quad (4)$$

The importance of such a definition arises as it correlates the annual thermal losses (Q_{loss}) with the maximum theoretical storage capacity (Q_{TES}). Thus, dynamic simulations are viable means to deliver the TES thermal losses that are strongly reliant on the boundary conditions (e.g. operation scenarios, TES geometry). The storage capacity is a function of the TES volume and the maximum and minimum temperature:

$$Q_{TES} = V \cdot \rho \cdot c_p \cdot (T_{max} - T_{min}) \quad (5)$$

Both definitions of TES efficiency are based on the 1st law of thermodynamics and, therefore, they do not consider the amount of the entropy produced over the TES operation. The entropy generation ultimately leads to lower the quality of the energy recovered and this arises due to the inherent irreversibility in recovering the energy input into the TES. One of the best examples of entropy generation is the decay of stratification over the storage period, which is often known as destratification. Therefore, it is of high importance to address a meaningful and rational measure that can

eliminate the pitfalls of the energetic efficiencies. Such a measure is the exergetic efficiency, which can be defined as the ratio of total exergy recovered from the TES to the total exergy input and can be expressed as below:

$$\psi = \frac{EX_{dis}}{EX_{ch}} \quad (6)$$

Another important measure is the amount of exergy destruction, which provides insights into the internal exergetic losses that play a major role in the destratification. Following an exergy balance:

$$\Delta EX = EX_{ch} - EX_{dis} - EX_{loss} - EX_{dest} \quad (7)$$

Where EX_{ch} , EX_{dis} and EX_{loss} are the charged exergy, discharged exergy total exergy losses (i.e. external losses), respectively. While EX_{dest} denotes the amount of exergy destruction (i.e. internal losses). Accordingly:

$$EX_{ch} = \rho \cdot \dot{V}_{w,ch} \cdot c_p \cdot \left[(T_{ch,in} - T_{ch,out}) - T_0 \cdot \ln \left(\frac{T_{ch,in}}{T_{ch,out}} \right) \right] \quad (8)$$

$$EX_{dis} = \rho \cdot \dot{V}_{w,dis} \cdot c_p \cdot \left[(T_{dis,out} - T_{dis,in}) - T_0 \cdot \ln \left(\frac{T_{dis,out}}{T_{dis,in}} \right) \right] \quad (9)$$

Where $T_{ch,in}$ and $T_{dis,in}$ represent the water inlet temperature during charging and discharging phases, respectively. Whilst $T_{ch,out}$ and $T_{dis,out}$ denote the water extraction temperature during charging and discharging modes, respectively. In this work, the initial soil temperature is the average ambient temperature (10 °C) and this implies that the reference environment (i.e. dead state) temperature (T_0) is equivalent to that of the soil temperature as it represents the undisturbed ground temperature and, thus, the undisturbed ground represents infinite heat sink, whose properties remain uninfluenced [37].

To achieve better stratification and higher TES efficiency, it is important to maintain the entropy generation as minimal as possible as it represents the amount of irreversibility exhibited by the TES system over the different operation phases. Thus, the minimization of entropy generation arises as a crucial tool for the examination of how efficient the considered TES system is. Following an entropy balance:

$$\dot{S} = (\dot{S}_{TES,in} - \dot{S}_{TES,out}) + \dot{S}_{Q_{loss}} + \dot{S}_{gen} \quad (10)$$

$$\Delta S = \rho \cdot c_p \int \frac{T}{T_0} \cdot dV = \rho \cdot c_p \int \frac{T(z)}{T_0} \cdot A_i \cdot dz_i \quad (11)$$

$$\dot{S} = \frac{dS}{dt} \quad (12)$$

Where ΔS , $\dot{S}_{TES,in}$ and $\dot{S}_{TES,out}$ represent the change in TES entropy generation rate, entropy rate of TES incoming flow and entropy rate of TES outgoing flow, respectively. Whilst $\dot{S}_{Q_{loss}}$ denote the entropy rate of TES external thermal losses that take place over the TES boundaries and flow toward the surroundings (e.g. ambient air or ground). The so-called entropy generation rate is given by \dot{S}_{gen} as it denotes the rate of entropy generation inherent in the TES system over the investigated period under the given set of boundary conditions.

Additionally, the water temperatures inside the TES plays a

critical role in the determination of TES performance and, thus, stratification plays a critical role in TES performance. As a result, the impact of TES geometry and dimensions on the stratification quality must be thoroughly evaluated. Under TES geometry and dimension, several factors can be listed: TES size, aspect ratio (H/d) and others. Thus, this work takes advantage of the stratification number and utilizes it to thoroughly examine the development and distribution of thermal segments inside the different large-scale TES geometries. This measure can be expressed as the quotient of the mean temperature gradients at any time to the maximum mean temperature gradient for the discharging/charging process [38], and given as follows:

$$Str(t) = \frac{\overline{(\partial T / \partial z)}_t}{\left(\overline{(\partial T / \partial z)}\right)_{\max}} \quad (13)$$

The numerator defines the mean of temperature gradients over a chosen process (e.g. charging or discharging), whereas the denominator exemplifies the maximum temperature gradient achieved during the process [19].

Another stratification measure is the stratification efficiency, which is based on MIX number and evaluates the moment of energy considering both of the temperature distribution and energy content of each individual segment in TES [39]. Accordingly, this number estimates how far is the investigated TES from a perfectly-stratified TES and it obeys the following [38]:

$$\eta_{Str} = 1 - MIX = 1 - \frac{M_E^{\text{stratified}} - M_E^{\text{exp}}}{M_E^{\text{stratified}} - M_E^{\text{fully-mixed}}} \\ = \frac{M_E^{\text{exp}} - M_E^{\text{fully-mixed}}}{M_E^{\text{stratified}} - M_E^{\text{fully-mixed}}} \quad (14)$$

Where the numerator represents the difference in moment of energy between the actual investigated TES and a fully-mixed one, whereas the denominator denotes the difference in moment of energy between a perfectly-stratified TES and a fully-mixed one. A main advantage of this number is that is a dimensionless number in which 1 represents a perfectly-stratified tank (unmixed), whilst a value of 0 indicates a fully-mixed tank [39]. The moment of energy can be calculated by integrating the sensible energy content of each segment along the height of the investigated TES and, then, the content of each segment is weighted with the height of its location height along TES vertical axis [26]. Accordingly:

$$M_E = \sum_{i=1}^n z_i \cdot Q_i = \sum_{i=1}^n z_i \cdot (\rho V_i) \cdot c_p \cdot T_i \quad (15)$$

3.3.2. Techno-economic analysis

In order to appropriately compare the different large-scale TES options, not only shall the technological development and materials advancement in their construction but also their associated capital and operation costs be included. Therefore, it is crucial to address a key indicator that reflects the advancement in the TES option together with the capital cost compared to another option. It is held that the leveled cost of stored heat (LCOS) is one of the key performance indicators that assists the planners to measure the TES performance from an economic perspective [40].

The method of the leveled cost of stored heat has become a very practical concept and valuable key to analyze different TES option for DH systems, especially those that are renewables-based. It is important to highlight that LCOS represents a comparative

indication on a cost-basis and does not represent a heat-supply tariff. The LCOS mainly results from the comparison of all costs that arise throughout the lifetime course of the TES operation. Thus, the LCOS is established as a benchmark for the assessment of techno-economic viability of different storage technologies ranking. The LCOS is defined as the quotient of the annualized total costs to the total amount of the discharged heat in the examined year and is expressed as follows:

$$LCOS = \frac{I_a + C_{O\&M} + c_{heat} \sum_{i=0}^t Q_{ch}(t) \cdot dt}{\sum_{i=0}^t Q_{dis}(t) \cdot dt} \quad (16)$$

Where the first term of the numerator (I_a) denotes the annualized TES CAPEX cashflow (capital expenditure in €/a), whereas $C_{O\&M}$ stands for the annual OPEX cash streams (operation and maintenance expenditure) and the last term ($c_{heat} \sum_{i=0}^t Q_{ch}(t) \cdot dt$) represents the cost of the total charged heat into the TES. Further, the denominator ($\sum_{i=0}^t Q_{dis}(t) \cdot dt$) expresses the total amount of discharged heat for the examined year. In order to annualize the total capital cost, it is essential to utilize the annuity factor:

$$I_a = I_{tot} \cdot \frac{i \cdot (1+i)^L}{(1+i)^L - 1} = I_{tot} \cdot ANF(i, L) \quad (17)$$

Herein, I_{tot} stands for the total investment cost of the TES installation (total CAPEX cashflow). Whereas i and L denote the nominal interest rate (3%) and the economic service life (i.e. 50 years), respectively.

For the maintenance and operation, the annual contribution is presumed to be a fixed fraction of 10% of the annualized CAPEX. The operation and maintenance cost includes the cleaning cost. Accordingly, the costs include the construction, operation and maintenance costs together with the total cost of the energy charged into the TES over the life cycle. It is important to mention that the CAPEX usually comprises the project decommissioning cost. Yet, this contribution is not considered in this study and this is due to the fact that such large-scale TES systems can be reutilized if some TES components (e.g. liners, diaphragm walls) are replaced with newer ones. Besides, the shallow pits can serve later as artificial lakes for urban areas and, thus, the decommissioning cost is neglected in this work. From an economic point of view, the LCOS method considers the most important players contributing to the economic evaluation of the investigated technology.

For the economic evaluation, the CAPEX is estimated considering the major contributions to the construction investment cost. Such contributions are the excavation, diaphragm wall, cut-off wall, insulation, liners, cover, plant construction and site facilities. In this work, the economic considerations are reproduced from Ref. [29] in order to evaluate the investment costs of large-scale TES and these considerations are based on realized projects and experience.

It must be pointed out that the volume specific excavation cost is independent of the TES height. Another note must be highlighted is the cost of the diaphragm wall is assumed to include the cost of anchors, which are frequently essential for construction of very large tank volumes ($>200,000 \text{ m}^3$) to provide stability. The anchors cost is assumed for the given boundary conditions of the soil. However, the cost might increase if the ground properties are different.

As this work does not consider a groundwater flow in the TES surroundings, the cost of the cut-off wall can be then excluded. Furthermore, it is held that the insulation installation in the side-walls is more challenging compared to that in the TES bottom and,

Table 5

Breakdown of the specific costs for the construction of seasonal TES (reproduced from Refs. [29,39]).

Contribution	(Specific) Costs	Remark
Excavation	20 €/m ³	Partly wet excavation
Diaphragm wall	550 €/m ²	50 m deep, (cost with anchors for the given soil)
Cut-off wall	50 €/m ²	In case of groundwater in 5 m distance
Sidewall	375 €/m ³	Insulation cost
	100 €/m ²	Insulation installation
Bottom	100 €/m ³	Insulation cost and installation (pressure resistant)
Liner	150 €/m ²	VA, Stainless steel (HT)
	50 €/m ²	Polymer liner (LT)
Cover	200 €/m ²	Floating cover (50 cm ins.)
	800 €/m ²	Trafficable floating cover
Plant construction	40,000 €	Independent TES construction
Site facilities	50,000 €	Fixed cost

therefore, the sidewall insulation encompasses two components; one is insulation volume dependent, while the other is dependent on the TES lateral area. Moreover, Table 5 reports the plant construction and site facilities as fixed costs and they are independent of the TES volume. However, it must be mentioned that the values reported in Table 5 are rough costs estimation based on experience, previous projects and literature.

It is noteworthy to mention that a steeper pit (e.g. height of 16.3 m instead of 10.5 m for a 100,000 m³) might lead to better feasibility in terms of economic considerations as demonstrated in Refs.[41] and [29]. As mentioned previously, the selection of the shallow pit dimensions in this work is to highlight its influence on the energetic and exergetic TES efficiency as well as the LCOS.

4. Techno-economic analysis: results and discussion

4.1. Estimation of TES specific investment cost

Fig. 8 compares the total specific investment cost for a single case without insulation and two other cases with insulation (i.e. 12 cm and 26 cm) for three TES options with a volume of 100,000 m³. Apparently, the special geotechnical works arise as the major contribution for the tank case and this is attributed to the necessity of providing stability to the vertical-walls TES. For the shallow pit, on the other hand, the special geotechnical works are not required and can be avoided and, thus, this contribution does not appear in the specific investment cost of the shallow pit. Yet, for shallow pits the major contribution comes from the cost of the lid (i.e. TES cover). Given the fact that shallow pits are realized with poor aspect ratios (H/d), those TES options tend to have larger top/bottom areas and, therefore, higher cover cost compared to other

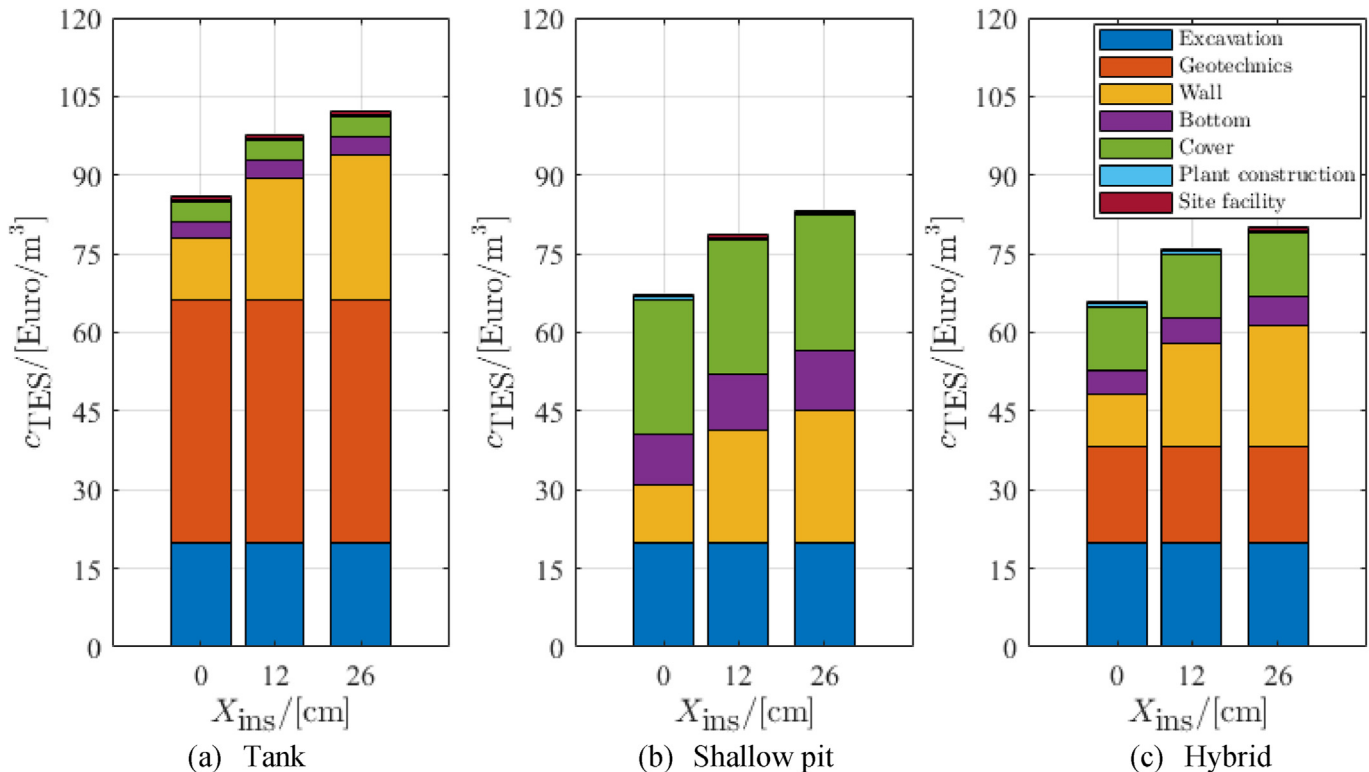


Fig. 8. Breakdown of the total specific cost for a 100,000 m³ TES installed in HT-DH according to the specific component costs in Table 5. (Geotechnics cost item refers to diaphragm wall installation, wall cost item refers to insulation cost and liner installations and bottom refers to the installation and cost of insulation and liner).

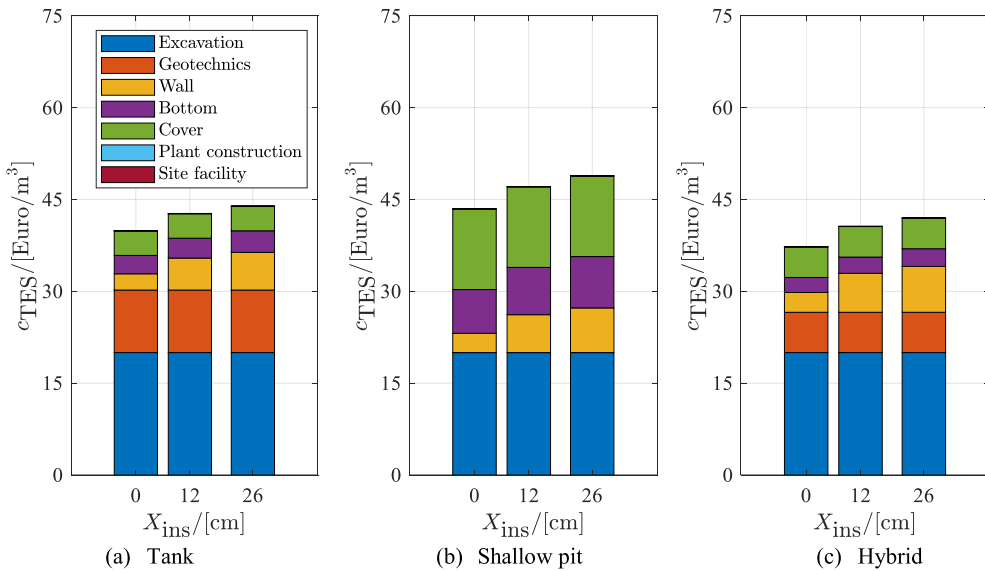


Fig. 9. Breakdown of the total specific cost for a 2,000,000 m³ TES installed in HT-DH according to the specific component costs in Table 5. (Geotechnics cost item refers to diaphragm wall installation, wall cost item refers to insulation cost and liner installations and bottom refers to the installation and cost of insulation and liner).

options. Whereas the hybrid TES option comprises both investment costs of special geotechnical works and cover with notable contribution. Yet, the wall insulation arises as the major contribution compared to other options (i.e. shallow pit and tank). Nevertheless, Fig. 8 addresses the hybrid TES as a promising solution given the economic considerations for the investigated volume as its specific investment cost is slightly lower compared to that of the shallow pit (For insulation thickness of 26 cm: $c_{\text{Hybrid}} = 80 \text{ €/m}^3$ and $c_{\text{Shallow-pit}} = 83 \text{ €/m}^3$).

Fig. 9 shows the contribution of each specific component in TES construction and implementation to the total specific cost of the tank (1), shallow pit (2) and hybrid (3) with a volume of 2,000,000 m³. Therein, the outcomes address the impact of economy-of-scale as the TES specific investment cost drastically decreases with increasing TES volume. Besides, Fig. 9 emphasizes that the tank of 2,000,000 m³ is cheaper than a corresponding shallow pit. This is due to the fact that expanding the shallow pit to larger volumes, the total surface area drastically increases compared to the tanks. Thus, noticeable is a rise in the costs of the cover, wall insulation and bottom insulation compared to those of the tanks.

4.2. Development of LCOS

Over the planning phase of a large-scale and/or seasonal TES, a substantial concern is usually paid to the start-up time of the TES until it reaches the quasi steady operation. Throughout this period, a large amount of thermal losses is usually lost in order to bring the surroundings ground (i.e. soil) from the initial temperature to a quasi-steady state temperature (i.e. higher temperature). Having considered an energy balance for the TES, this amount of losses has apparently an impact on the amount of heat delivered from the TES to the DH network. Consequently, this yields into an influence on the leveled cost of stored heat until it reaches the steady cost.

Fig. 10(a) depicts the decrease in the leveled cost of stored heat over 20 years of TES operation for a single case without insulation and two insulation thickness cases (i.e. 26 cm and 12 cm). It is obviously revealed that LCOS records higher values in the first 5 years and, then, the leveled cost drastically decreases following an exponential trend. In fact, this trend is due to the increase in the

discharged amount of heat from TES as illustrated from Fig. 10(b). The increase in the discharged amount of heat is attributed to the increase in the ground temperature as shown Fig. 11. Further, Fig. 10(a) reveals an average difference of appx. 10 €/MWh in the leveled cost of stored heat between the well-insulated case ($X_{\text{ins}} = 26 \text{ cm}$) and non-insulated case (0 cm) and this is due to the major contribution of the insulation material and installation in the lateral area of the TES to the total capital TES cost.

4.3. Impact of TES geometry and aspect ratio

The TES geometry plays a critical role in the decay of the stratification and this is due to the initiation of internal exergetic losses. Therefore, it is of high importance to guarantee an optimal choice for the TES geometry. Otherwise, higher energy losses and exergy losses are anticipated and performance might fall below expectations. Further, the geometry has an influence on the delivered amount of discharged heat and, thus, the leveled cost of the stored heat. In this regard, Fig. 12(a) compares the leveled cost of stored heat between three geometries (i.e. tank, conical shallow pit and hybrid). Undoubtedly, the shallow pit TES requires higher LCOS compared to the tank due to the performance fall exhibited by the shallow pit in terms of discharged heat as showed by Fig. 12(b). This LCOS difference highlights the tank outperformance in spite of the fact that construction of shallow pits is considered to be easily handled compared to the tanks since the installation of shallow pits does not involve special geotechnical works (i.e. diaphragm walls). Further, the excavation cost does not play a role in this scheme as it is related to unit volume instead of the unit length. Accordingly, it is of equal cost for both TES options. Moreover, the better performance of the tank is also attributed to lower values of SA/V ratio compared to that of the corresponding volume of shallow pit. As a result, the hybrid construction arises a feasible compromise that brings the benefits of both geometries (i.e. high efficiency of tanks and low specific costs of pits). Accordingly, Fig. 12 affirms the advantages of such a geometry as it results in lower LCOS compared to tanks and higher performance compared to pits.

Noticeable is the discharged amount of heat from the shallow pit is far lower compared to that of the tank and hybrid and this is undoubtedly related to the exergy consumption (i.e. exergy losses

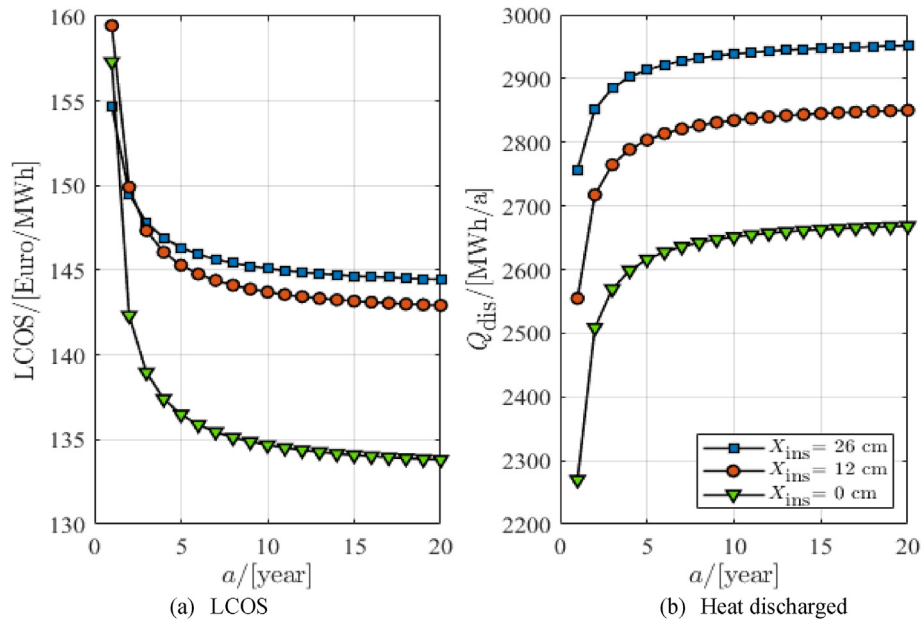


Fig. 10. Development of the levelized cost of stored heat and amount of discharged heat for a 100,000 m³ tank installed in HT-DH over 20 years of STES operation for 3 insulation thicknesses.

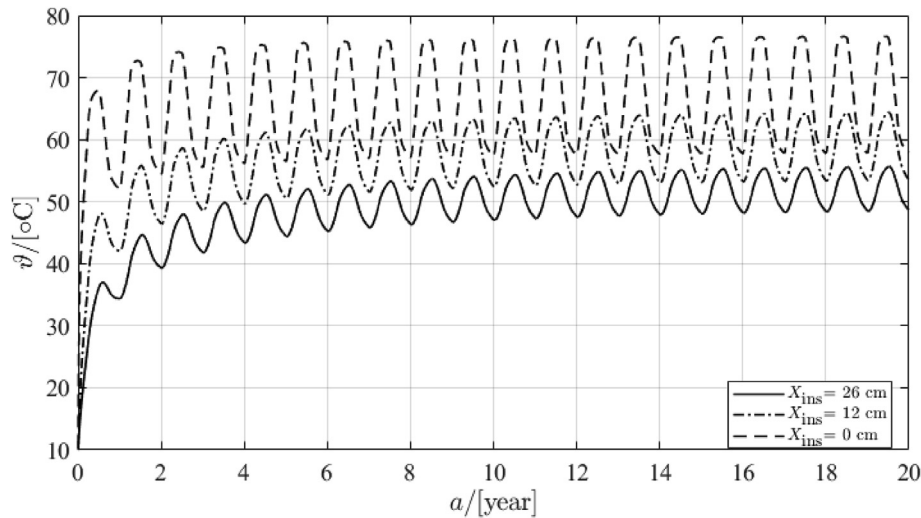


Fig. 11. Evolution of ground average temperature along the TES depth of 50 m and a distance of 1 m from the TES sidewalls for a 100,000 m³ tank installed in HT-DH over 20 years of STES operation for 3 insulation thicknesses.

and exergy destruction) in the shallow pit over the annual operation. Consequently, the shallow pit supplies heat with lower quality compared to other geometries (i.e. tank and hybrid). Herein, the increase in the total exergy loss of the shallow pit is strongly attributed to the inherent irreversibilities during both storage and discharging phases. Thus, the shallow pit exhibits lower exergetic efficiency as revealed by Fig. 13(b). In other words, the TES was charged with high exergy heat, whereas discharged with lower exergy quality due to the increase in the total exergy losses (i.e. internal and external losses). Further, Fig. 13(a) points out that the installation of more insulation slightly lowers the amount of exergy input and, simultaneously, increases the quality of exergy supplied. Besides, Fig. 13 confirms the feasibility of a hybrid TES geometry in terms of exergy analysis as it shows that such a geometry has higher exergy efficiency compared to a shallow pit.

A crucial aspect for a good stratification is the TES shape (i.e. aspect ratio) because an improper TES height-to-diameter ratio might increase the internal exergetic losses resulting in an enhancement of mixing and, thus, stratification decay. Consequently, the following section elaborates the tank aspect ratio influence on the LCOS, exergy consumption and stratification quality. For the investigation, the insulation thickness of the lateral sidewalls was set to 26 cm (i.e. with insulation) and 0 cm (without insulation). On the other hand, the insulation thickness variation took place for the TES cover. Fig. 14 exhibits that tanks with aspect ratios of ($H/d = 0.25$) tend to have high exergy destruction and, thus, higher total exergy losses compared to other options. Accordingly, the exergy efficiency is at its lowest with such aspect ratio ($H/d = 0.25$). Whereas the exergy efficiency increases as the aspect ratio increases. In this context, an aspect ratio of ($H/d = 3$)

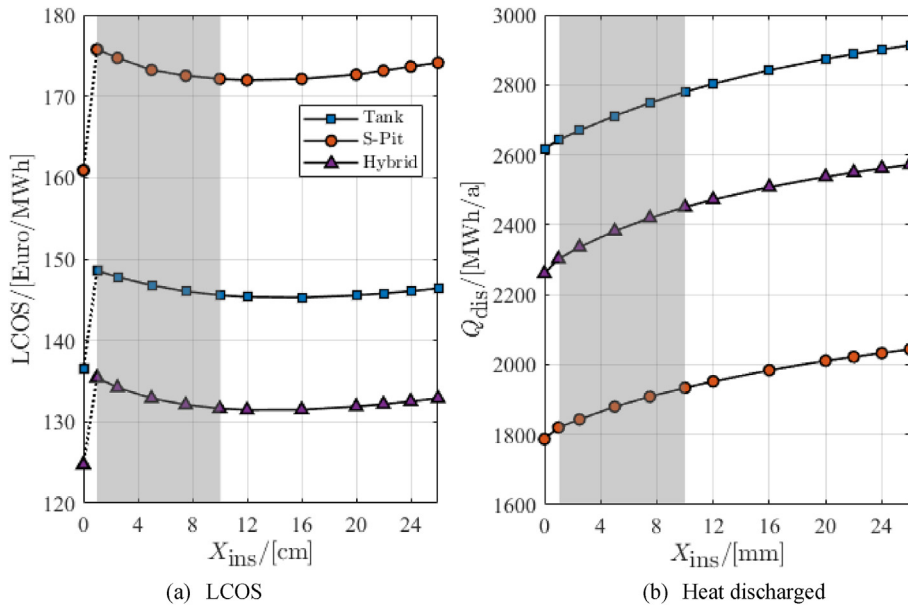


Fig. 12. Comparison of the leveled cost of stored heat and the discharged amount of heat over insulation thickness for different TES geometries with a volume of 100,000 m³ and same amount of available heat. (Note: the grey-shaded region represents only a theoretical range as such small insulation layers are unpractical).

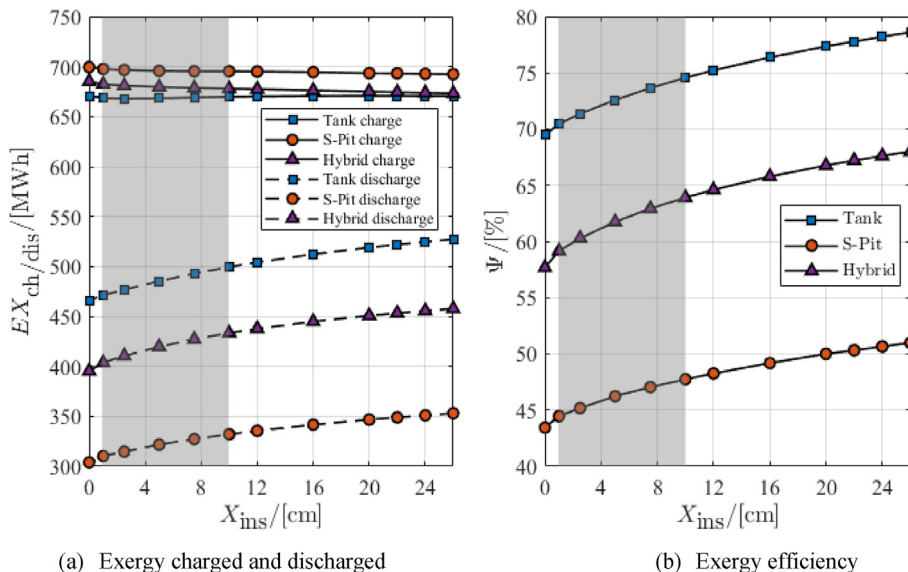


Fig. 13. Exergy charged, discharged and efficiency for 3 TES geometries (tank, shallow pit and hybrid) with a volume of 100,000 m³ and same amount of charged heat. (Note: the grey-shaded region represents only a theoretical range as such small insulation layers are unpractical).

has the lowest exergy destruction compared to other aspect ratios. Further, it is notable that as the aspect ratio lies in the range of ($H/d = 1\text{--}3$), the exergy efficiency tends to be similar with semi-equivalent values and, therefore, it is held that increasing the aspect ratio ($H/d > 1$) does not bring any further improvements on the tank performance. Besides, given some economic constraints, the maximum feasible depth for a buried tank is limited to 50 m below ground; subsequently, this excludes configurations with ($H/d > 1$) since the excavation below 50 m is not feasible. (See Fig. 25 in Appendix for the non-insulated case).

Since the case of ($U_{top} = 0.1$ W/(m².K)) presents the most promising results for the different insulation thicknesses of the cover, it is chosen for further techno-economic analysis. Despite the increase in performance accompanied by the increase in aspect

ratio, Fig. 15 reveals that this increase triggers the leveled cost of stored heat to rise as well. Accordingly, the stored heat unit price increases by 13.5 €/MWh, if an aspect ratio ($H/d = 1$) is selected instead of ($H/d = 0.25$). Then, the stored heat unit price might further increase by additional 23 €/MWh, if an aspect ratio ($H/d = 2$) is chosen. This increase in the stored heat unit price is greatly attributed to the drastic increase in the special geotechnical works required for the TES sidewalls. Therefore, it is recommended to avoid depths below 50 m since it might lead to the economic infeasibility.

To inspect the role of geometry on TES stratification, several measures are often utilized to exemplify the stratification development and decay throughout the different TES operation phases (e.g. charging, standby). The majority of these measures are TES

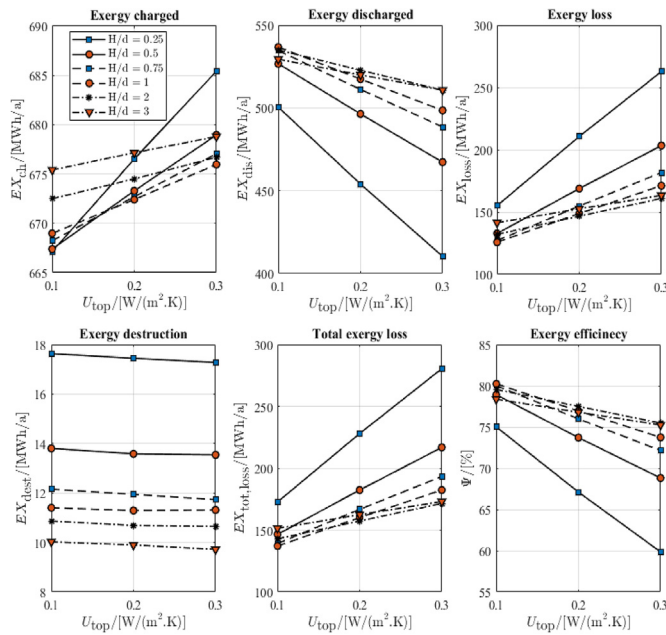


Fig. 14. Exergy analysis for a 100,000 m³ tank with insulation over the lateral sidewalls and bottom for different aspect ratios.

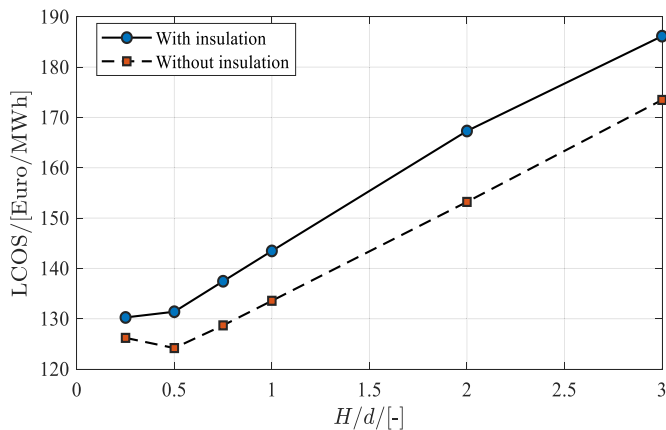


Fig. 15. The leveled cost of stored heat over the aspect ratio for a tank with a volume of 100,000 m³ and $U_{\text{top}} = 0.1 \text{ W}/(\text{m}^2 \cdot \text{K})$.

temperature-dependent, i.e. the stratification measures consider the TES temperature at each TES segment as function of TES height over the entire operation period. Therefore, it is crucial to firstly introduce and compare the development of TES temperatures for the different geometries considered in this work. Consequently, Fig. 16 emphasizes the role of TES geometry in terms of temperature for different TES shapes (i.e. tank with $H/d = 1$, shallow pit and hybrid) with a volume of 100,000 m³. Herein, the TES temperature is compared at specific locations. One location is at the very top of the TES, the second is at a height at which the TES volume is halved (i.e. 50,000 m³) and the last point at the TES very bottom. Fig. 16 demonstrates that the tank with aspect ratio of 1 outperforms the other TES geometries as the temperatures (top, mid and bottom) remain at higher levels compared to other geometries. In particular, the tank geometry is capable of maintaining high temperature during the standby phase compared to the shallow pit. This means less buoyancy-induced mixing and, therefore, better stratification quality compared to the shallow pit. Whilst the hybrid

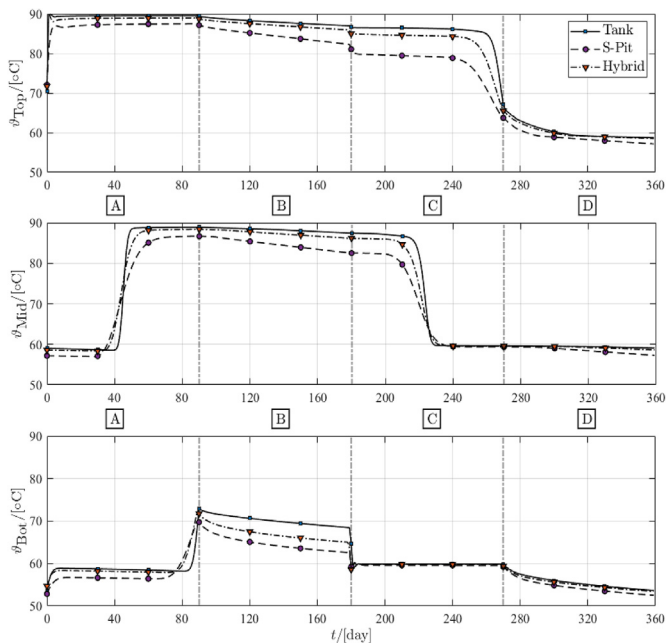


Fig. 16. Evolution of TES temperature at three locations (top, middle and bottom) over the 5th year for a 100,000 m³ TES with $U_{\text{top}} = 0.1 \text{ W}/(\text{m}^2 \cdot \text{K})$ and insulation thickness of 26 cm for the TES bottom and sidewalls. Mid refers to the location at which the TES has its half volume (i.e. 50,000 m³).

geometry represents a geometrical compromise between the tank and the shallow pit. Moreover, Fig. 17 illustrates the reason behind the selection of a tank with ($H/d = 1$) for the comparison as it has a slight increase in the top temperature compared to other aspect ratios. It is important to mention that the comparison of tank temperatures (bottom and tank half volume) are not considered for the comparison in Fig. 17 as they do not significantly differ. In addition, Figs. 16 and 17 show 4 operation phases for the TES that: charging, standby, discharging and idle, which correspond to A, B, C and D, respectively.

Fig. 18 exemplifies the development of stratification number and stratification efficiency for a 100,000 m³ tank with 4 aspect ratios, a shallow pit and a hybrid. In this context, four TES operative phases are clearly recognized that are: charging, standby, discharging and idle. Undoubtedly, it is revealed that a tank shape with ($H/d = 1$) exhibits the best stratification quality compared to other options. It also has less surface area and, consequently, less thermal loss. Thereby, this tank has higher quality of energy delivered to DH in terms of temperature. Whereas the aspect ratio ($H/d = 0.25$) has the poorest stratification quality among the set of tank cases. This is attributed to the tank height and the large cover area leading to higher amount of annual thermal losses. Compared to the tank configurations, the shallow pit appears the least stratification efficiency as it falls down to 60% during charging and discharging phases. The hybrid configuration, on the other hand, is held to be a moderate option between the tank and pit as it shows better stratification compared to that of the shallow pit. This outcome comes in accordance with the outcomes shown in Fig. 13(b).

Fig. 18 depicts that TES stratification quality tends to decrease over the 1st half of charging phase in terms of stratification efficiency and, then, it increases indicating a good stratification quality. This phenomenon can be justified as during the 1st half of charging period, more than half of TES volume is filled with water at approximately 55 °C (initial temperature) and, simultaneously, 90 °C hot water is injected from the top diffuser. Whereas in the 2nd half of period A, more than half of TES volume is filled with hot

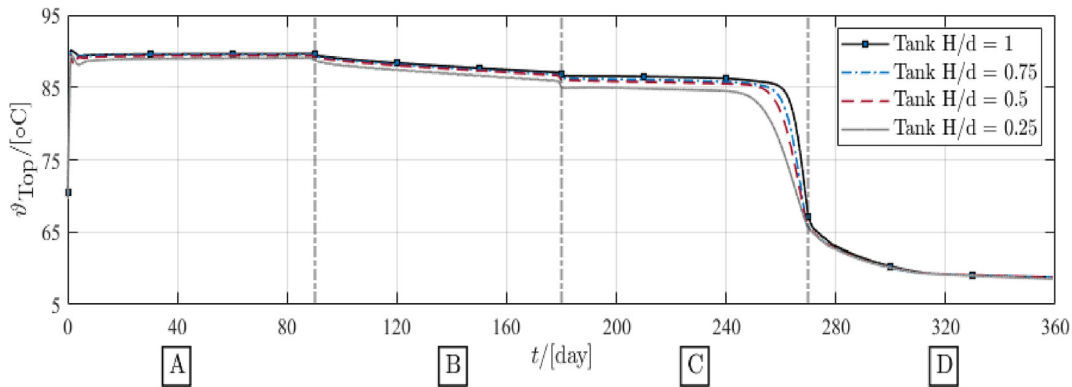


Fig. 17. Evolution of top temperature over the 5th year for a 100,000 m³ tank with different aspect ratios (H/d = 0.25, 0.5, 0.75 and 1), $U_{\text{top}} = 0.1 \text{ W}/(\text{m}^2 \cdot \text{K})$ and insulation thickness of 26 cm for the TES bottom and sidewalls.

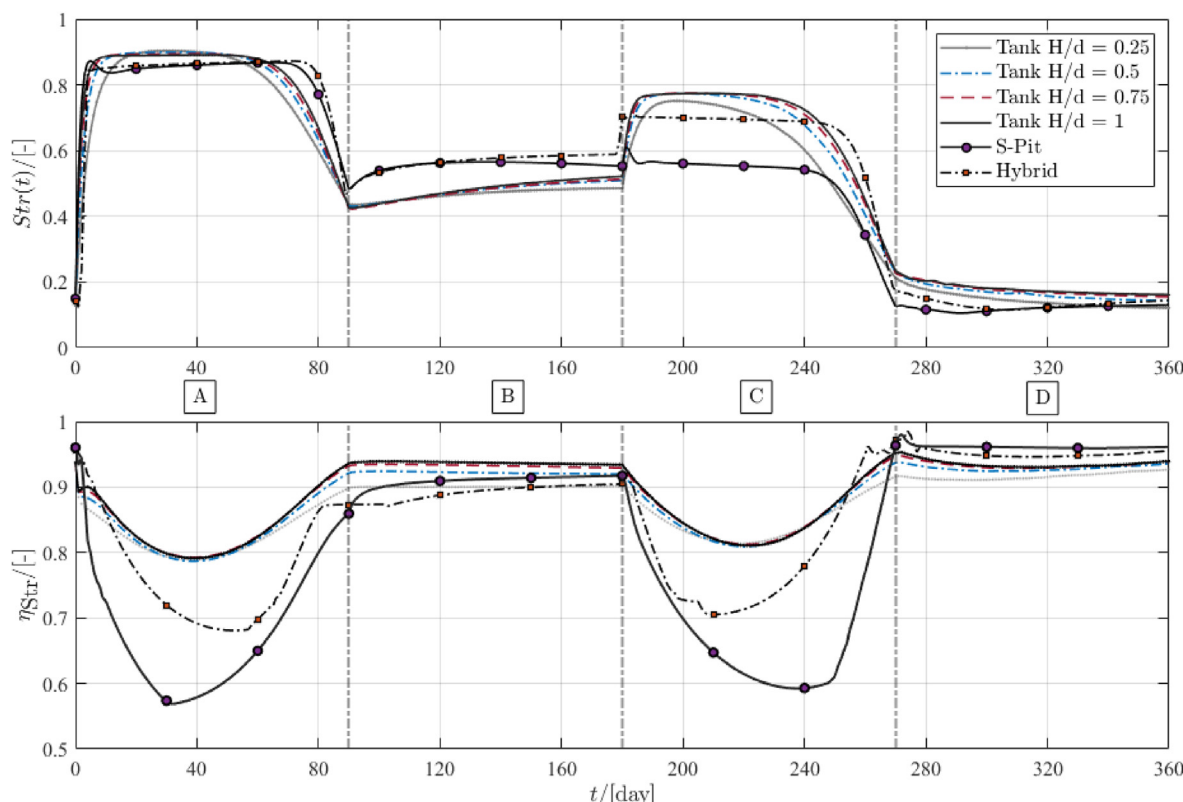


Fig. 18. Stratification number and stratification efficiency development over the 5th year for a 100,000 m³ TES with $U_{\text{top}} = 0.1 \text{ W}/(\text{m}^2 \cdot \text{K})$ and insulation thickness of 26 cm for the TES bottom and sidewalls.

water and, meanwhile, charging carries on. Both other options (shallow pit and hybrid) reveal similar phenomenon and trend. However, the shallow pit and hybrid suffer severe decline in stratification quality compared to the tank during A. This is attributed to the fact that the hybrid and shallow pit have larger lateral area and, accordingly, higher thermal losses. Yet, it must be pointed out that the hybrid option has moderate stratification quality compared to the shallow pit.

In the region (B), TES undergoes a standby mode in which no incoming/outgoing flowrates and, therefore, stratification maintains a good quality with a slight decay attributed to the thermal losses from TES envelope. Besides, TES experiences a buoyancy-driven heat flow over the standby mode and, subsequently,

mixing is enhanced. Over this period, TES with aspect ratio of (H/d = 1) exhibits a notable stratification quality compared to other aspect ratios. Notable is the increase in stratification efficiency for the shallow pit and hybrid due to the top thermal losses because of the large top area.

Throughout the region (C), TES discharges the stored energy to R-DH network and is injected with 60 °C water from the return line. Therefore, the stratification quality suddenly experiences a decline due to the extraction of hot water from the upper diffuser and, simultaneously, injection of lukewarm water with 60 °C from the bottom diffuser. Thus, the stratification progressively develops leading to an increase in stratification quality by the end of this phase for the tanks. On the other hand, the shallow pit

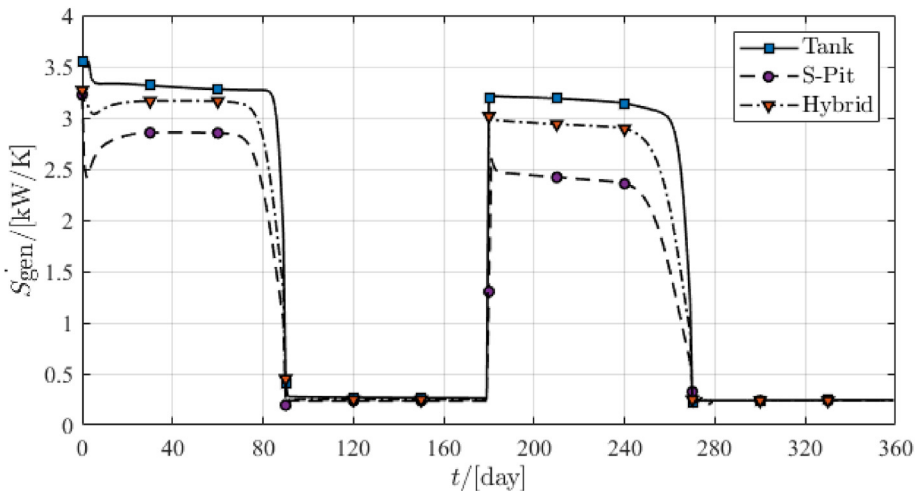


Fig. 19. Rate of the entropy generation due to TES internal losses for three TES geometries: tank with AR = 1, S-Pit and hybrid configurations over the 5th year for a 100,000 m³ TES with $U_{top} = 0.1 \text{ W}/(\text{m}^2\cdot\text{K})$ and insulation thickness of 26 cm for the TES bottom and sidewalls.

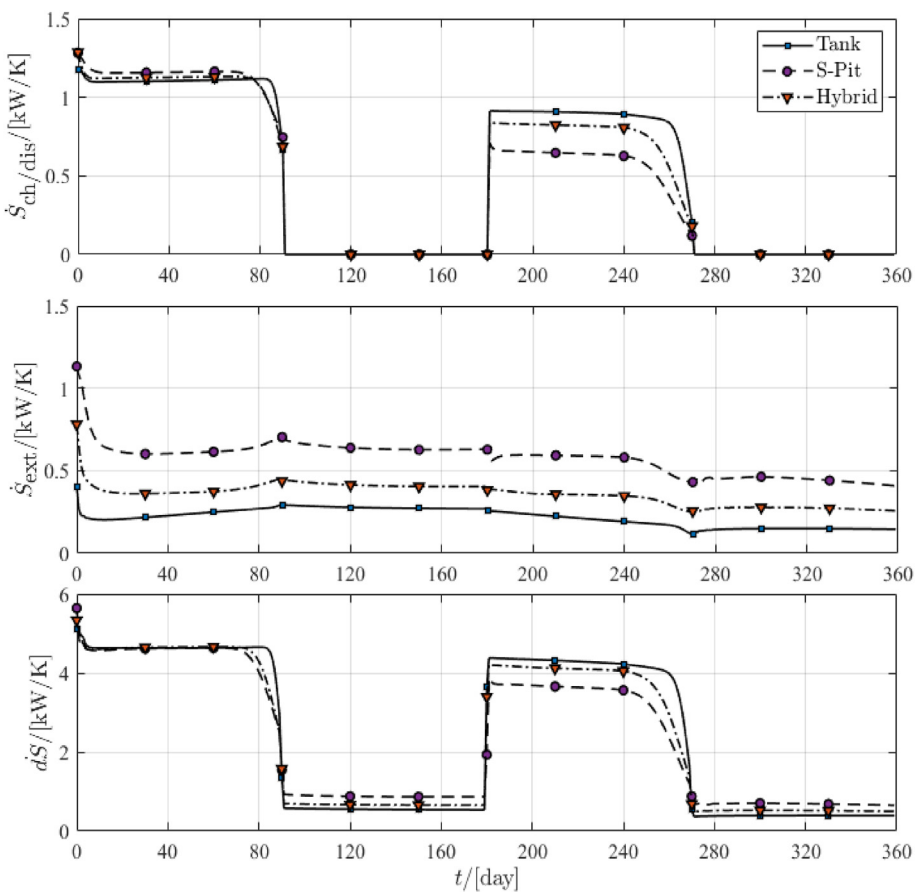


Fig. 20. Rate of the entropy (charged/discharged, external losses and change) for three TES geometries: tank with AR = 1, S-Pit and hybrid configurations over the 5th year for a 100,000 m³ TES with $U_{top} = 0.1 \text{ W}/(\text{m}^2\cdot\text{K})$ and insulation thickness of 26 cm for the TES bottom and sidewalls.

experiences a decrease in the stratification quality resulting in the poorest quality compared to other options. Remarkable is the stratification quality of hybrid TES, which arises as a compromise between the tank and the shallow pit.

Period (D) is similar to period (B) whereby conductive heat transfer is dominating with no incoming and outgoing flowrates. Therefore, this period is characterized with initial mixing that is

promptly counterbalanced by buoyancy-driven mixing in order to avoid misleading results by inverse thermocline. Yet, the high level of stratification is also attributed to thermal losses that bring the TES to lower temperatures compared to that of DH return temperature.

Figs. 19 and 20 shows the rate of entropy generation due to the internal losses for the three examined TES geometries; tank,

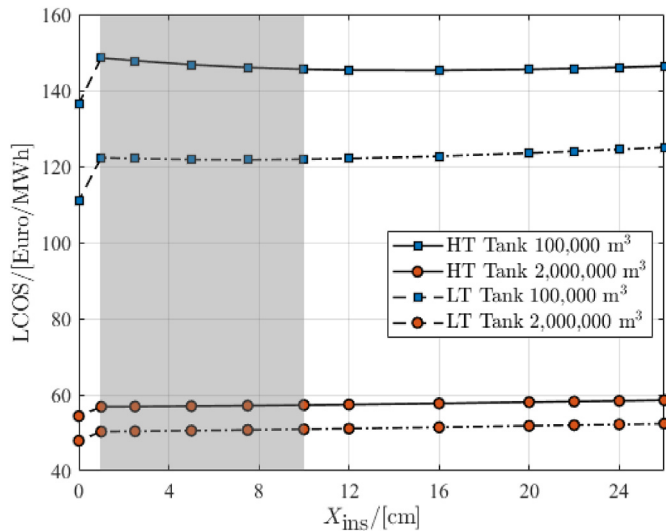


Fig. 21. Evolution of the tank LCOS and performance over different insulation thicknesses in low- and high-temperature DH systems for two TES volumes; 100,000 m³ and 2,000,000 m³. (Note: the grey-shaded region represents only a theoretical range as such small insulation layers are unpractical).

shallow pit and hybrid. Therein, it is important to distinguish between the dynamic TES phases that include incoming/outgoing enthalpy rates and the stationary phases (i.e. standby and idle). During the charging phase, the considered TES geometries exhibit the same trend for the rate of entropy generation. Nevertheless, the tank TES continues to generate entropy until the end of this phase compared to the shallow pit, whilst the hybrid TES shows an intermediate level between both options with approximation to tank. This phenomenon observed in the tank (i.e. the continuous entropy generation) is due to the capability of the tank to achieve higher TES temperatures due to better SA/V compared to other options. Whilst the shallow pit has lower temperature at the end of the charging phase. This fact is a key as it demonstrates that the tank has better TES capacity and stores higher amount of energy compared to the shallow pit. The hybrid, on the other hand, is considered as a

valuable compromise. Over the discharging course, notable is the highest rate of entropy generation for the tank compared to others as it is also longer. This is similar to the phenomenon observed during the charging phase, which is attributed to the tank capability of achieving high temperatures and maintaining better stratification.

Throughout the standby phases, the three TES geometries show similar rate of entropy generation. These two phases are characterized with low rate of entropy generation compared to charging/discharging phases and this can be justified by the fact that standby phases have no enthalpy rates. Thus, the entropy balance considers only the thermal losses and the internal losses due to irreversibilities. Accordingly, there is always a notable decrease in the TES temperature at the upper part enhancing the mixing and, therefore, lower temperature and poor stratification quality.

It is important to point out that the tank exhibits higher generation rate of entropy due to the high stratification quality. This outcome affirms that the shallow pit has the poorest stratification quality as illustrated in Fig. 18. Having considered stratification measures and entropy generation, it must be pointed out that a tank with ($H/d = 1$) exhibits the premium stratification quality among other options. It also has less surface area and, consequently, less thermal loss. Such a tank has higher quality of energy delivered to DH in terms of temperature.

4.4. Impact of the DH characteristics

It is held that there exist many factors (i.e. temperature, flow-rates and heat source) that influence the operation of the seasonal TES at the DH level. In this context, one of the key milestones for R-DH is lowering the operation DH temperature range in order to achieve higher system performance. Having considered that, it is worthwhile to examine the influence of the DH temperature on the leveled cost of the heat. Thus, two representative DH characteristics were considered; a low-temperature DH (LT-DH) system with a heat pump whereby the supply and return temperatures were 80 °C and 30 °C, respectively. Whilst the other was a high-temperature (HT-DH) system in which 90 °C/60 °C were assigned as supply and return temperatures, respectively. Since the aim is to provide an in-depth understanding to the DH characteristics

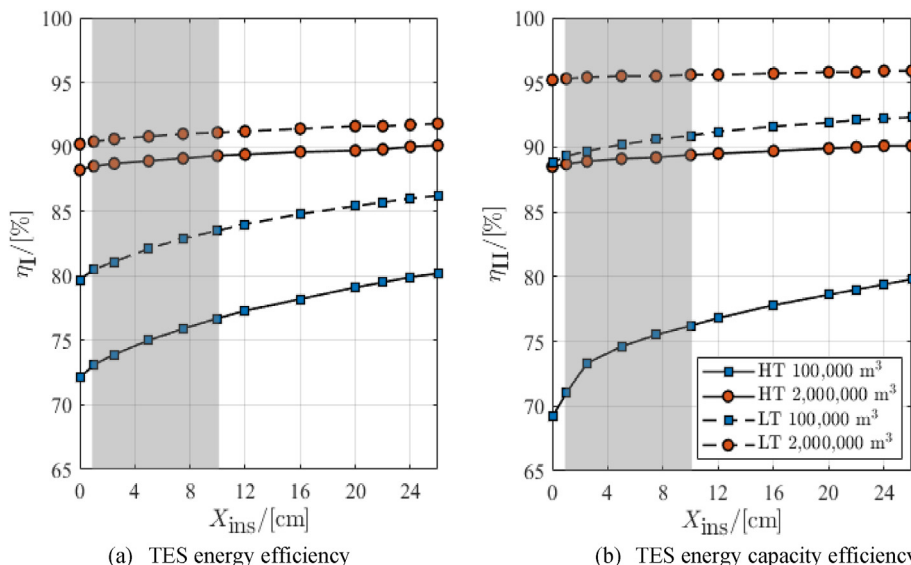


Fig. 22. Evolution of the TES performance over different insulation thicknesses in low- and high-temperature DH systems for two TES volumes; 100,000 m³ and 2,000,000 m³. (Note: the grey-shaded region represents only a theoretical range as such small insulation layers are unpractical).

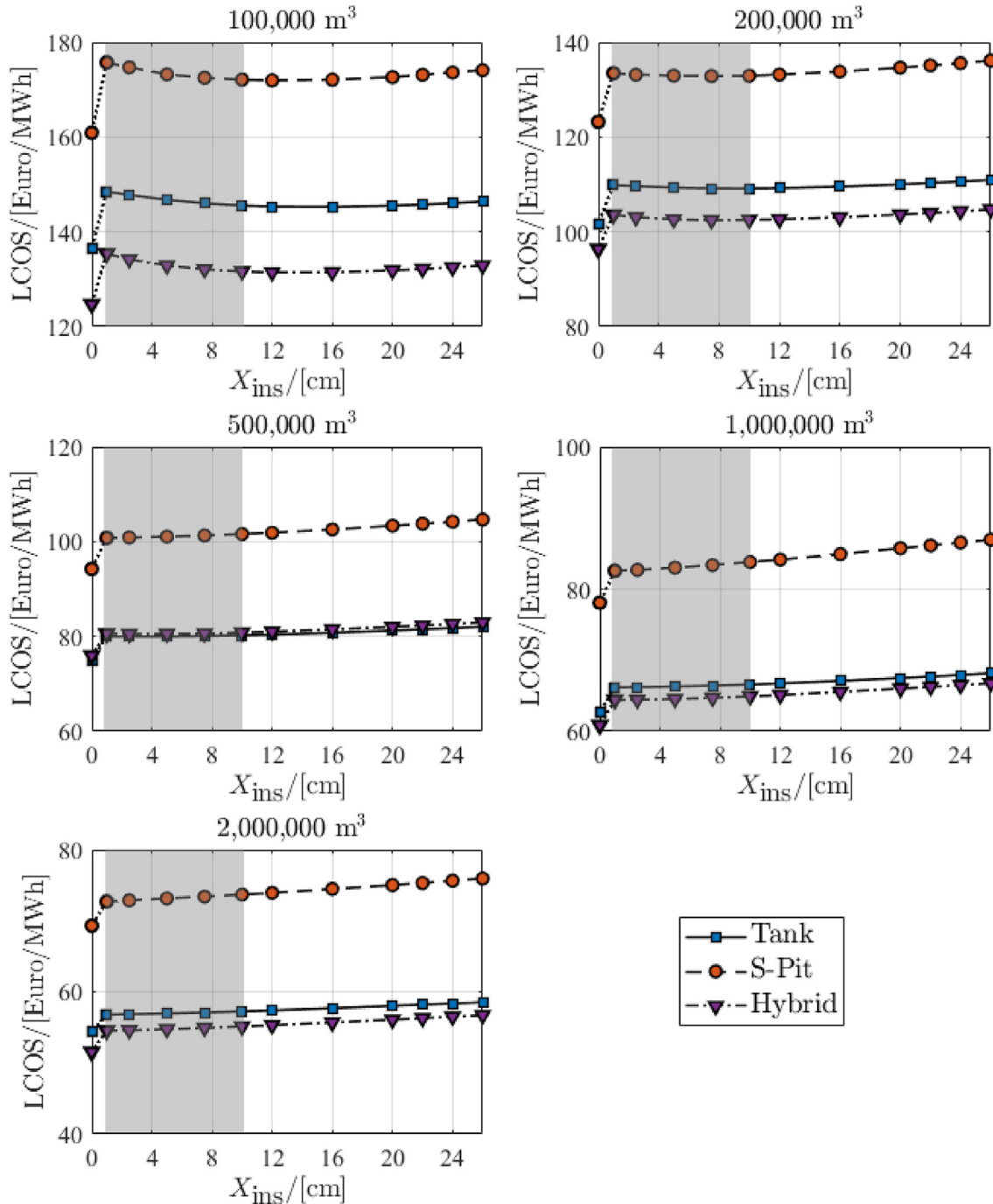


Fig. 23. Comparison of the leveled cost of stored heat over insulation thickness for different TES geometries (tanks, shallow pits and hybrids) with different volumes for HT-DH systems. (Note: the grey-shaded region represents only a theoretical range as such small insulation layers are unpractical).

influence, it is essential to maintain same heat input to the TES. In other words, the charged energy into the LT TES should be equivalent to that of the HT TES in order eliminate the influence of the lower/higher energy input on the LCOS.

Fig. 21 shows a comparison between two tank volumes ($100,000 \text{ m}^3$ and $2,000,000 \text{ m}^3$) installed in HT-DH and LT-DH and under same boundary conditions (e.g. ground thermal properties, TES energy input). Besides the lower thermal losses, the LT-DH system brings further benefits such as lowering the LCOS due to the increase in the discharged amount of heat out of the TES. Another advantage is that such systems as they operate at lower

temperatures ($<90^\circ\text{C}$), they do not require the installation of stainless-steel liners, which is often seen costly (150 €/m^2). Instead, it is sufficient to install polymer liners with resistance to temperatures up to 85°C and such liners are more feasible under these terms (50 €/m^2). Therefore, a decrease of approx. 25 €/MWh is achieved if a transition from a HT-DH to LT-DH is planned and conducted. Whereas this difference is reduced to approx. 10 €/MWh if the TES volume increases up to $2,000,000 \text{ m}^3$. This low difference is attributed to lower contribution of the liner cost in the total investment cost compared to the case of $100,000 \text{ m}^3$. Another reason is that at volumes of $2,000,000 \text{ m}^3$ the performance

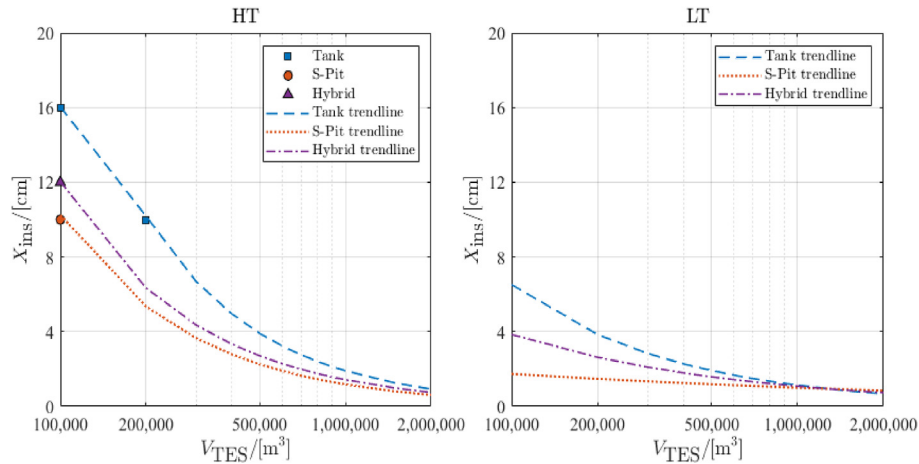


Fig. 24. Optimal insulation thickness with respect to LCOS for the insulated TES volumes and geometries considered in this work.

difference between tanks in LT-DH and those in HT-DH notably decreases to lower than 6% as demonstrated by Fig. 22, whilst it is in the range of 8% up to 18% for the 100,000 m³ tank. Furthermore, it is worthwhile to point out that the increase in the LT TES performance is mainly justified to lower thermal losses and higher storage capacity as the temperature difference is 50 K instead of 30 K as it is the case with HT TES. Subsequently, this also has an impact on the levelized cost of stored heat.

4.5. Impact of the TES volume

The increase in the TES volume results in lowering the TES thermal losses as the surface area-to-volume ratio gets smaller. Another outcome originates from the economic point of view, it is essential to exploit the specific cost reduction with increasing TES volume. Thus, the larger the TES size, the cheaper the specific TES cost. Fig. 23 elaborates the impact of TES size increasing on the LCOS for the TES geometries (i.e. tank, shallow pit and hybrid). Noticeable is the LCOS for the shallow pit is higher compared to that of the tank and hybrid in spite of the volume investigated. The reason behind is that the tanks and hybrids achieve better (SA/V) ratio leading eventually to fewer thermal losses and, subsequently, a higher amount of discharged heat. On the other hand, as the shallow pits size increases, the top and bottom areas then drastically increase compared to the other geometries. Eventually, this will yield a higher specific cost for the bottom insulation and lid in the shallow pit compared to other geometries as shown in Figs. 8 and 9. Subsequently, the LCOS of the shallow pits increases surpassing the LCOS of the corresponding volume of the tanks due to the enormous increase in the capital cost, while maintaining poor performance. Moreover, it must be pointed out that for a volume of 100,000 m³, the hybrid geometry exhibits the lowest LCOS. This trend is notable for all other volumes but with less slight difference to the LCOS of tanks. This key outcome reveals the importance of such a geometry consideration when planning large-scale TES. It must be suggested that the hybrid geometry is a promising compromise between the tanks and pits as it has low LCOS and high technical performance.

In this regard, Fig. 24 summarizes the optimal insulation thickness with respect to LCOS for the volumes investigated and geometries considered in this work following the analysis conducted in the preceding sections. In order to name a candidate thickness as optimal value, it should deliver the lowest LCOS among the set of the solutions with insulation. Besides, it is crucial to underline that an insulation thickness below 10 cm will be likely

not installed. Therefore, a limit of 10 cm (dotted line) is plotted to examine whether a case (depending on geometry, volume and DH temperature) has an insulation thickness beyond 10 cm, then this stands for its optimal. Otherwise, all thicknesses below 10 cm are disregarded and it is deemed better to keep the TES uninsulated.

Fig. 24 reveals that there is an optimal insulation thickness in the range of (12 cm–16 cm) for a 100,000 m³ TES installed in HT systems. For larger TES volumes, however, the thickness values notably drop below the limit. Furthermore, Fig. 24 highlights a key message that it might be useful to leave the TES systems installed in LT uninsulated as the all thickness values are below 10 cm. Despite the aforementioned outcomes, it must be concretely pinpointed that the cases investigated do not consider groundwater flow in the TES surroundings. It is crucial to underline that the insulation becomes crucial for the TES system when the groundwater tables are present nearby the buried TES systems. The importance of the insulation is to preserve the groundwater quality prescribed by national standards as emphasized in Ref. [34].

5. Conclusions

The planning and construction of the large-scale thermal energy storage (TES) systems is often seen as a cumbersome process due to the wide list of factors that have to be considered. Thus, this work made efforts to tackle the planning challenges in a techno-economic analysis framework in order to establish the planning guidelines for large-scale TES. In this context, the work numerically investigated the role of the TES geometry, TES volume and DH characteristics supported by numerical simulations. The investigation considered several performance indicators that are based on either 1st law or 2nd law of thermodynamics. Due to its importance in technology ranking, the work also carried out a techno-economic analysis using the levelized cost of stored heat (LCOS).

As for the TES geometry, the outcomes suggested the out-performance of the tank shape compared to the shallow pit. Several performance measures (i.e. energy efficiency, energy capacity efficiency and exergy efficiency) emphasized a notable increase in TES efficiency when a tank shape was considered. Compared to the shallow pit, the tank has smaller surface and, consequently, lower thermal losses. As a result, the stratification tends to be more effective for a tank TES as demonstrated by means of the stratification number and stratification efficiency. Thanks to its high performance, the tank has lower values for LCOS compared to that of the shallow pit. Yet, the shallow pit is characterized with its low specific investment cost. Thus, the work attempted to obtain the

advantages of both TES geometries and, accordingly, planned a third TES geometry named as hybrid TES. In this regard, the results underlined the features of this geometry as it has performance approaching that of the tank TES but with lower investment cost resulting in the lowest LCOS.

Not only the economy-of-scale phenomenon was notable as the TES volumes increased but also the performance notably increased. The outcomes demonstrated the role of TES volume in increasing the TES performance. Besides, the results suggested that as the TES volumes increases, the role of the insulation thickness becomes insignificant on the efficiency and LCOS given the fact that no optimal insulation thickness was found for volumes ($>200,000 \text{ m}^3$). Yet, the insulation is an essential component if the TES surroundings contain groundwater flow.

The work also investigated the role of the TES operation temperature and the results underlined that a transition to low-temperature DH system led to a significant increase in TES efficiency (i.e. energy and exergy) and, hence, lower levelized cost of stored heat compared to TES installed in high-temperature DH systems. Yet, the outcomes pointed out that no optimal insulation thickness was found for the LT-TES in case insulation is needed (see Fig. 24). However, the insulation remains a crucial component for the TES systems if groundwater flow is observed. Hence, future work should focus on materials and methods for cost-efficient approaches for insulating underground TES.

Moreover, previous works from the authors showed that the pit outperforms the tank in terms of the economic considerations only. In this context, the non-insulated pit has better feasibility than the insulated pit. Whereas the tank with insulation outperforms the non-insulated tank. Thus, the authors in this work chose specific dimensions for the shallow pit in order to highlight the influence on TES efficiency (energetic and exergetic) and, accordingly, the LCOS.

CRediT authorship contribution statement

Abdulrahman Dahash: Conceptualization, Methodology, Software, Visualization, Formal analysis, Writing – original draft.
Fabian Ochs: Funding acquisition, Writing – review & editing.
Alice Tosatto: Writing – review & editing.

Declaration of competing interest

The authors declare that they have no known competing financial interests or personal relationships that could have appeared to influence the work reported in this paper.

Acknowledgements

This project is financed by the Austrian “Klima-und Energiefonds” and performed in the frame of the program “Energieforschung”. It is part of the Austrian flagship research project “Giga-Scale Thermal Energy Storage for Renewable Districts” (giga_TES, Project Nr.: 860949). Therefore, the authors wish to acknowledge the financial support for this work.

A. Appendix

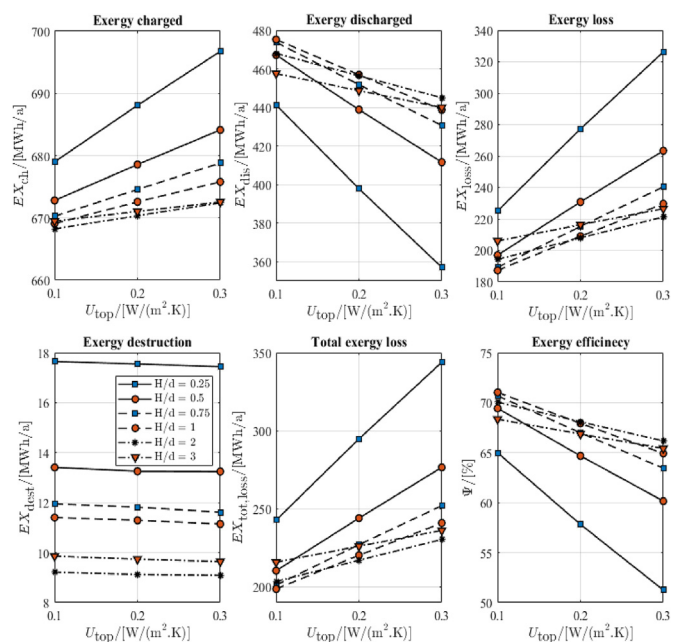


Fig. 25. Exergy analysis for a $100,000 \text{ m}^3$ tank without insulation over the lateral sidewalls and bottom with a volume of $100,000 \text{ m}^3$ and different aspect ratios.

References

- [1] E. Commission, Clean energy for all Europeans Package, Directorate—General for Energy (European Commission) (2019).
- [2] W. Zappa, M. Junginger, M. van den Broek, Is a 100% renewable European power system feasible by 2050? *Appl. Energy* 233 (234) (2019) 1027–1050.
- [3] G. Pfeßmann, P. Blechinger, How to meet EU GHG emission reduction targets? A model based decarbonization pathway for Europe's electricity supply system until 2050, *Energy Strategy Reviews* 15 (2017) 19–32.
- [4] F. Robertson Munro, P. Cairney, A systematic review of energy systems: the role of policymaking in sustainable transitions, *Renew. Sustain. Energy Rev.* 119 (2020).
- [5] M. Child, C. Kemfert, D. Bogdanov, C. Breyer, Flexible electricity generation, grid exchange and storage for the transition to a 100% renewable energy system in Europe, *Renew. Energy* 139 (2019) 80–101.
- [6] An EU strategy for heating and cooling: communication from the commission to the European parliament, the council, the European economic and social committee and the committee of the regions, European Commission, Brussels, Belgium, 2016.
- [7] E. Commission, A Roadmap for Moving to a Competitive Low Carbon Economy in 2050, European Commission, 2011.
- [8] D. Ürge-Vorsatz, L.F. Cabeza, S. Serrano, C. Barreneche, K. Petrichenko, Heating and cooling energy trends and drivers in buildings, *Renew. Sustain. Energy Rev.* 41 (2015) 85–98.
- [9] International Energy Agency (IEA), Transition to Sustainable Buildings: Strategies and Opportunities to 2050, Organisation for Economic Cooperation and Development (OECD), Paris, France, 2013.
- [10] E.E. Agency, Energy efficiency and energy consumption in the household sector, European Environment Agency, 2017. Last modified on.
- [11] H. Averfalk, S. Werner, Economic benefits of fourth generation district heating, *Energy* 193 (2019).
- [12] H. Dorotić, T. Pukšec, N. Duić, Multi-objective optimization of district heating and cooling systems for a one-year time horizon, *Energy* 169 (2019) 319–328.
- [13] C. Brunner, G. Deac, S. Braun, C. Zöphel, The future need for flexibility and the impact of fluctuating renewable power generation, *Renew. Energy* 149 (2020) 1314–1324.
- [14] M. Liebensteiner, M. Wrienz, Do intermittent renewables threaten the electricity supply security? *Energy Econ.* (2019).
- [15] J.M. Jebamalai, K. Marlein, J. Laverge, Influence of centralized and distributed thermal energy storage on district heating network design, *Energy* 202 (2020).
- [16] F. Levihn, CHP and heat pumps to balance renewable power production: lessons from the district heating network in Stockholm, *Energy* 137 (2017) 670–678.
- [17] M. Victoria, K. Zhu, T. Brown, G.B. Andresen, M. Greiner, The role of storage technologies throughout the decarbonisation of the sector-coupled European energy system 201, *Energy Conversion and Management*, 2019.
- [18] A.L. Reed, A.P. Novelli, K.L. Doran, S. Ge, N. Lu, J.S. McCartney, Solar district heating with underground thermal energy storage: pathways to commercial

- viability in North America, *Renew. Energy* 126 (2018) 1–13.
- [19] A. Dahash, F. Ochs, M. Bianchi Janetti, W. Streicher, Advances in seasonal thermal energy storage for solar district heating applications: a critical review on large-scale hot-water tank and pit thermal energy storage systems, *Appl. Energy* 239 (2019) 296–315.
- [20] M.H. Abokersh, M. Vallès, L.F. Cabeza, D. Boer, A framework for the optimal integration of solar assisted district heating in different urban sized communities: a robust machine learning approach incorporating global sensitivity analysis, *Appl. Energy* 267 (2020).
- [21] R. Renaldi, D. Friedrich, Techno-economic analysis of a solar district heating system with seasonal thermal storage in the UK, *Appl. Energy* 236 (2019) 388–400.
- [22] T. Yang, W. Liu, G.J. Kramer, Q. Sun, Seasonal thermal energy storage: a techno-economic literature review, *Renew. Sustain. Energy Rev.* 139 (2021).
- [23] A. Dahash, M. Bianchi Janetti, F. Ochs, Numerical analysis and evaluation of large-scale hot water tanks and pits in district heating systems, *Building Simulation 2019 Conference*, Rome (Italy), 2019, 02–04 September 2019.
- [24] T. Schmidt, T. Pauschinger, P.A. Sørensen, A. Snijders, R. Djebbar, R. Boulter, J. Thornton, Design aspects for large-scale pit and aquifer thermal energy storage for district heating and cooling, *Energy Procedia* 149 (2018) 585–594.
- [25] T. Pauschinger, T. Schmidt, P.A. Soerensen, A. Snijders, R. Djebbar, R. Boulter, J. Thornton, Integrated cost-effective large-scale thermal energy storage for smart district heating and cooling. Design aspects for large-scale Aquifer and pit thermal energy storage for district heating and cooling, International Energy Agency Technology, 2018.
- [26] A. Dahash, F. Ochs, A. Tosatto, W. Streicher, Toward efficient numerical modeling and analysis of large-scale thermal energy storage for renewable district heating systems, *Appl. Energy* 279 (2020).
- [27] Underground Thermal Energy Storage (UTES) - state-of-the-art, example cases and lessons learned, in: A.J. Kallesøe, T. Vangkilde-Pedersen (Eds.), *GEOTHERMICA – ERA NET Cofund Geothermal* (2019).
- [28] K. Narula, F. de Oliveira Filho, W. Villasmil, M.K. Patel, Simulation method for assessing hourly energy flows in district heating system with seasonal thermal energy storage, *Renew. Energy* (2019).
- [29] F. Ochs, A. Dahash, A. Tosatto, M. Bianchi Janetti, Techno-economic planning and construction of cost-effective large-scale hot water thermal energy storage for Renewable District heating systems, *Renew. Energy* 150 (2019) 1165–1177.
- [30] V. Panthalookaran, W. Heidemann, H. Müller-Steinhagen, A new method of characterization for stratified thermal energy stores, *Sol. Energy* 81 (8) (2007) 1043–1054.
- [31] C. Chang, B. Nie, G. Leng, C. Li, X. She, X. Peng, J. Deng, Influences of the key characteristic parameters on the thermal performance of a water pit seasonal thermal storage, *Energy Procedia* 142 (2017) 495–500.
- [32] D. Park, H.-M. Kim, D.-W. Ryu, B.-H. Choi, C. Sunwoo, K.-C. Han, The effect of aspect ratio on the thermal stratification and heat loss in rock caverns for underground thermal energy storage, *Int. J. Rock Mech. Min. Sci.* 64 (2013) 201–209.
- [33] E. Hahne, Y. Chen, Numerical study of flow and heat transfer characteristics in hot water stores, *Sol. Energy* 64 (1–3) (1998) 9–18.
- [34] A. Dahash, F. Ochs, G. Giuliani, A. Tosatto, Understanding the interaction between groundwater and large-scale underground hot-water tanks and pits, *Sustain. Cities Soc.* 71 (2021).
- [35] A. Dahash, M. Bianchi Janetti, F. Ochs, Detailed axial symmetrical model of large-scale underground thermal energy storage, *Proceedings of the 2018 COMSOL Conference*, Lausanne (Switzerland), 2018, pp. 22–24. October 2018.
- [36] A. Dahash, M. Bianchi Janetti, F. Ochs, Numerical heat transfer modeling of large-scale hot water tanks and pits, in: *Proceedings of Eurotherm Seminar #112: Advances in Thermal Energy Storage*, Lleida, Spain, 2019.
- [37] H. Torío, D. Schmidt, Development of system concepts for improving the performance of a waste heat district heating network with exergy analysis, *Energy Build.* 42 (10) (2010) 1601–1609.
- [38] M.Y. Haller, C.A. Cruickshank, W. Streicher, S.J. Harrison, E. Andersen, S. Furbo, Methods to determine stratification efficiency of thermal energy storage processes – review and theoretical comparison, *Sol. Energy* 83 (10) (2009) 1847–1860.
- [39] A. Dahash, F. Ochs, A. Tosatto, Simulation-based design optimization of large-scale seasonal thermal energy storage in renewable-based district heating systems, in: *Proceedings of BauSIM 2020 (Virtual): 8th Conference of IBPSA Germany and Austria*, Graz, Austria, 2020.
- [40] A. Smallbone, V. Jülich, R. Wardle, A.P. Roskilly, Levelised cost of storage for pumped heat energy storage in comparison with other energy storage technologies, *Energy Convers. Manag.* 152 (2017) 221–228.
- [41] Abdulrahman Dahash, Ph.D. thesis work. Insights into Large-Scale Seasonal Hot-Water Tanks and Pits: Modelling, Techno-Economic Analysis and Optimization, University of Innsbruck, 2021.